



Urban Aerial Mobility for airport shuttle service

Di Lv ^a, Wei Zhang ^a, Kai Wang ^{a,*}, Han Hao ^a, Ying Yang ^b

^a School of Vehicle and Mobility, Tsinghua University, 100084 Beijing, China

^b School of Management, Shanghai University, 200444 Shanghai, China



ARTICLE INFO

Keywords:

Urban aerial mobility

eVTOL

Airport shuttle

Facility location

ABSTRACT

Airport shuttle service is regarded as one of the most promising use cases for the early deployment of Urban Air Mobility (UAM). This study introduces an integrated modeling framework for UAM-based airport shuttles. The framework covers strategic decisions, including site selection, route planning, fleet size design, and station capacity design, as well as operational considerations such as demand estimation, service level determination, and scheduling. This framework aims to provide UAM stakeholders with an optimization and management solution that incorporates the above integrated decisions. Through a case study at Beijing Capital International Airport, several notable findings emerge: (1) UAM demonstrates feasibility in airport shuttles, offering a minimum 28.4% reduction in travel time while maintaining costs comparable to alternative modes. (2) The system exhibits robustness and high service quality, effectively accommodating 94.8% of reserved orders and 90.7% of ad-hoc orders. (3) Larger-capacity eVTOLs (e.g., 5–6 passengers) are well-suited to expedite UAM deployment for airport shuttle services. (4) Emphasizing the importance of vehicle performance, a high cruise speed correlates with revenue growth approximating linear progression, highlighting its significance for the advancement of UAM. These findings enhance our understanding of UAM's potential in airport shuttle services and offer valuable insights for UAM stakeholders.

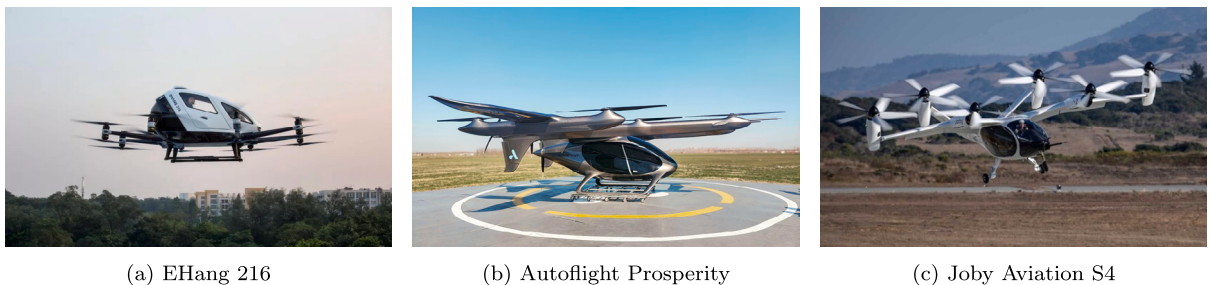
1. Introduction

Over the next three decades, a significant shift towards urbanization is expected, with the urban population projected to increase from 56% in 2021 to an estimated 68% by 2050. Urbanization has a substantial impact on economic growth, providing access to various trade, healthcare, and educational resources, along with convenient services for the population. However, it also brings forth a critical challenge: traffic congestion, leading to environmental pollution, financial losses, and traffic accidents (Rassafi and Vaziri, 2005; Gudmundsson et al., 2016; Heidorn, 2018; Biehle, 2022). As an illustrative example, during the peak of the COVID-19 pandemic in April 2020, reduced travel in Europe resulted in a 17% reduction in carbon emissions (IEA, 2020) and a 36% decline in traffic-related fatalities for that month (Briefing, 2020). Meanwhile, in Asia, productivity losses due to traffic congestion have caused economic losses ranging from 2% to 5% of GDP (Habitat, 2022). In the latter part of the 20th century, Tokyo, known for its high population density, grappled with severe traffic congestion. Over four decades, it made significant progress in developing an advanced rail transit system, additional transportation routes, and well-planned urban zoning. However, this progressive approach had its drawbacks, including high costs and lengthy implementation periods (Okamoto and Makino, 2007; Xing et al., 2010; Zhou and Gao, 2020).

Urban Air Mobility (UAM) is gaining momentum as it seeks to transform urban transportation from a two-dimensional to a three-dimensional paradigm (Holden and Goel, 2016; National Academies of Sciences et al., 2020; McKinsey, 2022). UAM envisions

* Corresponding author.

E-mail address: cwangkai@tsinghua.edu.cn (K. Wang).



(a) EHang 216

(b) Autoflight Prosperity

(c) Joby Aviation S4

Fig. 1. Symbol eVTOL prototypes.

leveraging underutilized low-altitude urban airspace to offer flexible, user-friendly door-to-door travel services. The key to this transformation is the emergence of new electric vertical takeoff and landing (eVTOL) aircraft technology (see Fig. 1) (EHang Intelligence, 2021; Autoflight-Press, 2021; Joby-Aviation, 2023). These aircraft are electrically powered and capable of vertical takeoff and landing on flat terrain.

EVTOLs mark a transformative step forward in aviation, offering significant advantages over traditional helicopters in terms of safety, noise reduction, and cost-effectiveness. Safety stems from distributed electric propulsion, which involves the use of multiple small, independently powered rotors. This design enhances safety by ensuring that the aircraft can maintain stability and continue flying even if some rotors fail. For instance, the Velocity model features 18 rotors, while the Lilium Jet is equipped with 33 ducted fans. Additionally, certain models incorporate both rotors and wings, enabling them to glide in emergency situations, further enhancing safety. The reduction in noise levels makes eVTOLs particularly well-suited for urban environments. For example, the Joby S4 produces cruising noise of only 45 dB at an altitude of 500 meters (Joby-Noise, 2022), and Archer's model is reported to have a noise level of 45 dB at 2000 ft, making them approximately 1000 times quieter than helicopters (Archer, 2022). From a cost perspective, eVTOLs are also more economical over their lifecycle. According to analyses by Deloitte, McKinsey, NASA, and Uber, the cost of eVTOL services is projected to range from \$2.5 to \$6.25 per person per mile in the initial phases, with the potential to decrease to \$0.5 to \$3.75 in the medium to long term (Berckman et al., 2022; Johnston et al., 2020; Hamilton, 2018; Holden and Goel, 2016). This is significantly lower than the cost of helicopter services, which stand at approximately \$15 per mile. The collective optimism about UAM based on eVTOL technology underscores the potential for these aircraft to revolutionize short-distance air travel, making it safer, quieter, and more affordable.

With the continued advancement of eVTOL vehicles, UAM is seen as a promising solution to alleviate ground traffic congestion (Wang and Qu, 2023). By 2035, a substantial market, comprising 200,000 eVTOL vehicles valued at 320 billion USD, is anticipated to emerge (Grandl et al., 2018). Various applications of UAM, including inner-city air taxis, airport shuttles, intercity transport, medical emergencies, and tourist sightseeing, offer pragmatic avenues for UAM implementation (Straubinger et al., 2020; Cohen et al., 2021).

Simultaneously, airport shuttles play a vital role in the adoption of UAM (Shaheen et al., 2018; Goyal et al., 2018; Mayor and Anderson, 2019; Hader et al., 2020; Fu et al., 2022). Traditional airport shuttle modes fall into low-capacity options (e.g., taxis, ride-sharing, private vehicles) and high-capacity means (e.g., buses, subways, airport rail lines, and airport buses). They can also be categorized based on transportation and service attributes into private transportation, offering speed and comfort but with the risk of delays due to congestion, and public transportation, cost-effective and reliable yet slower on average, less comfortable, and lacking door-to-door service. Air travelers often face the need for punctuality, and UAM's attributes, including flexibility, reliability, and transportation efficiency, position it as a promising solution for airport shuttles.

Several UAM projects are underway, signaling a significant move towards airport shuttle services. In a notable development, Joby Aviation finalized a deal with Dubai in February 2024 to launch UAM services by 2026. This initiative includes constructing a vertiport at Dubai International Airport to facilitate seamless connections between the airport and vital city areas such as the city center, ports, and resort zones (Joby-UAE, 2024). Joby Aviation's eVTOL has also successfully completed the third stage of FAA certification, marking a critical step towards operational readiness (Joby-Certification, 2024). Volocopter is setting its sights on a high-profile demonstration at the Paris Olympics, working in collaboration with the Paris Airport Group and the French Civil Aviation Authority to establish a link between Paris Charles de Gaulle Airport and Bourget Airport (Volocopter-Paris, 2023). Further bolstering its credentials, Volocopter received an extension of its production organization approval from the German Federal Aviation Authority in February 2024 (Volocopter-POA, 2024). UrbanV, a consortium created by Rome Airport, Venice Airport, Nice Côte d'Azur Airport, and Bologna Airport, aims to integrate technology for efficient UAM services. It is reported that shuttle services connecting Rome Fiumicino Airport with the city center are slated to commence by the end of 2024 (UrbanV, 2024). These projects illustrate the growing momentum and collaborative efforts to make UAM a reality for airport shuttle services.

As UAM has yet to gain widespread commercialization, pilot projects for airport shuttles often focus on specific routes of limited scale, leaving many questions about operational intricacies unanswered. Key issues such as shuttle station locations, the extent of air travelers' demand, the required number of eVTOL aircraft, and flight scheduling for balancing reliability and cost-effectiveness need immediate attention (Vascik et al., 2018; Ravich, 2019; Yedavalli and Mooberry, 2019; Hill et al., 2020; Vempati et al., 2022).

Our research aims to assess the feasibility of implementing UAM for airport shuttles. We have developed a comprehensive decision-making framework covering demand estimation, site selection, route planning, fleet sizing, station capacity, and scheduling. This framework spans both strategic and operational levels, addressing the dynamic interaction between passengers and operators to provide an efficient management solution for UAM in the context of airport shuttles. The primary contributions of this study are as follows:

- We present a comprehensive decision framework and operational management plan for UAM airport shuttle services to streamline integrating this innovative system into existing urban transport networks.
- We construct a mixed-integer linear programming model that outlines the infrastructure deployment, the supply–demand relationship between operators and customers, and the operational service processes of the system, providing a methodology for managing UAM services.
- We demonstrate the economic feasibility and the benefits for citizens in accessibility by implementing UAM for airport shuttle services, using Beijing Capital International Airport as a case study.
- An in-depth analysis of the network's performance reveals that eVTOLs with fixed-wing configurations, characterized by larger payloads and higher cruising speeds, significantly improve network balance and cost-effectiveness.

The remainder of this paper is organized as follows: Section 2 provides a summary of existing UAM research. Section 3 outlines the service processes and framework of UAM in airport shuttle scenarios. In Section 4, we establish an optimization mathematical model for the integrated decision framework. Section 5 presents our research findings based on the case study of Beijing Capital International Airport and analyzes the results. Finally, in Section 6, we conclude the paper and offer insights into future directions.

2. Literature review

UAM emerges as a pivotal solution for clean and efficient transportation, aimed at revolutionizing door-to-door transit within urban environments. Despite its potential, the path to its development is fraught with challenges including infrastructure limitations, regulatory barriers, concerns over noise pollution, and safety issues (Binder et al., 2018; Becker et al., 2018; Al Haddad et al., 2020; Cho and Kim, 2022). Nevertheless, there is a growing interest in leveraging UAM for seamless airport-to-city connections, positing airport shuttle services as a vital stepping stone towards the broader adoption of UAM technologies. The capabilities of eVTOL aircraft, particularly their high-speed performance and suitability for operation over less densely populated areas, make them an attractive option for time-sensitive travelers.

Currently, the Vertical Flight Society has cataloged over 800 models of eVTOLs, which utilize multiple rotors or ducted fans and are categorized into three main types: Wingless, “Lift+Cruise”, and Vectored Thrust (Vertical Flight Society, 2023). Wingless eVTOLs are characterized by their smaller size and lighter weight, performing well in ascent and descent but offering a limited range of around 50 km and a speed of approximately 100 km/h. “Lift+Cruise” eVTOLs combine vertical and horizontal momentum with a fixed wing, resulting in cruise speeds ranging from 120 km/h to 200 km/h. Vectored Thrust eVTOLs adjust propulsion elements at different flight stages, achieving higher speeds of 150 km/h to 250 km/h. Both “Lift+Cruise” and Vectored Thrust eVTOLs boast extended endurance with mileage capabilities ranging from 100 km to 250 km.

Surveys reveal a substantial interest in UAM for airport shuttles, positioning it as a highly favored mode of transport, second only to air taxis, and preferred over autonomous driving solutions (Shaheen et al., 2018). This scenario is anticipated to play a significant role in UAM's revenue generation, suggesting airport shuttles could contribute to over half of UAM's long-term income (Hader et al., 2020). Multi-agent simulation studies validate the feasibility of integrating multiple service routes connecting to airports (Fu et al., 2022), with optimistic outlooks on the efficiency, security, and scalability of eVTOL services (Goyal et al., 2018; Mayor and Anderson, 2019).

Before UAM can transition into commercial operations, accurate demand estimation is crucial for stakeholders to assess feasibility, guide infrastructure and service planning, and formulate safety standards. Various research methods, including surveys, economic analysis, modeling, and simulation, have been employed. Notably, Binder et al. (2018), Cho and Kim (2022), and Hwang and Hong (2023) used stated preference surveys to investigate key factors influencing UAM market share. While SP surveys can reveal passengers' preferences and behaviors, the public's lack of understanding of UAM may lead to subjective biases. To refine demand estimations, various transportation and aviation analytical methods have been applied. Becker et al. (2018) employed a gravity model calibrated with smartphone and population density data, while Fu et al. (2022) used multi-agent simulation, and Goyal et al. (2018) utilized Monte Carlo simulation to gain insights into UAM demand. These methods rely on extensive, high-quality data and can be challenging to interpret. Moreover, gravity models may not suit varying scenarios. Pattern selection models have become popular tools for analyzing UAM market potential, using criteria such as income level, time efficiency, and cost to make informed evaluations (Haan et al., 2021; Vascik and Hansman, 2017; Rimjha et al., 2021a; Wai et al., 2021). Although capturing dynamic changes is difficult, these models have been widely used and validated in transportation with high predictive accuracy. Additionally, current demand estimations predominantly focus on the passenger perspective, overlooking the interplay between demand estimation and planning or operational decision-making.

Vertiports play a crucial role in enabling eVTOL aircraft operations, providing facilities for take-off, landing, charging, and maintenance. The strategic selection of vertiport locations is instrumental in optimizing travel routes, enhancing service quality, and minimizing urban impact. Current research methodologies, including clustering, geographic analysis, and multi-objective optimization, focus on demand, distance, and cost as key factors for comprehensive evaluation and optimization (Bulusu et al., 2021;

Peng et al., 2022; Tarafdar et al., 2019; Wei et al., 2020). Additionally, considerations around capacity constraints, noise pollution, and the integration of existing helicopter infrastructure are pivotal in assessing vertiport viability in urban settings (Peng et al., 2022; Robinson et al., 2018; Ribeiro et al., 2023). Several studies have explored vertiport location optimization at the network and system levels. Willey and Salmon (2021) employed optimization techniques focusing on hub location and subgraph isomorphism. Venkatesh et al. (2020) tackled station capacity and network traffic balance, while Feldhoff and Soares Roque (2021) introduced a ranking system that evaluates accessibility and applicability. Despite these advancements, there is a need for a more integrated approach to vertiport planning and analysis for the relationships between infrastructure, demand-supply dynamics, and vehicle performance.

UAM is poised to operate at high densities and on a large scale, necessitating meticulously designed operational plans for its safe and efficient implementation. Optimization techniques are pivotal in this context, guiding critical decisions that encompass factors such as charging protocols, energy availability, and weather conditions, all of which significantly influence flight safety (Husemann et al., 2023; Chan et al., 2023; Kleinbekman et al., 2020). The efficacy of UAM services is heavily reliant on efficient operational management, highlighting the urgency of employing advanced fleet management, planning, and scheduling strategies to save passenger wait times (Wang et al., 2022a; Wu and Zhang, 2020; Kim, 2019; Wei et al., 2021). In addressing the challenges of emergency procedures, Wei et al. (2022) explored the use of mixed-integer linear programming to identify alternative landing sites for eVTOLs, enhancing safety protocols during critical scenarios. Further contributing to the operational framework, Wang et al. (2022b) synthesized factors such as the number, location, and capacity of airports with fleet management strategies, introducing an adaptive discretization technique aimed at optimizing operational outcomes. The operational intricacies of UAM encompass a wide array of elements, from vehicle performance and flight path planning to scheduling. The goal is to forge UAM safer, more efficient and broadly accessible.

The airport shuttle service represents a specialized segment of UAM. Brunelli et al. (2023) utilized a Stated Preference survey to identify key factors such as income, travel frequency, and a propensity towards ride-sharing as significant influences on the adoption of UAM airport shuttle services. Meanwhile, Roy et al. (2021) adopted a mode selection methodology to estimate demand, facing limitations related to the consideration of existing helipads as potential locations and the lack of detailed operational strategies. Choi and Park (2022) introduced a tiered pricing model, albeit with the limitation of assuming passenger departure from fixed points like Seoul Station, which may not accurately capture diverse passenger preferences. Lewis et al. (2021) discussed the interplay between upfront costs, average accident intervals, annual profits and round-trip traffic, yet did not extend these insights into a tangible operational framework. Focusing on Los Angeles, Rimjha et al. (2021b) applied a demand-centric clustering analysis, but did not adequately address operational intricacies and capacity issues. Rath and Chow (2022)'s revenue maximization study primarily contended with taxi services without adequately considering limitations on site capacities. Roy et al. (2022) explored a multicommodity network flow model, but the analysis was constrained by a small dataset (with a fleet size of five), raising questions about the findings' generalizability. Overall, while there is growing research on UAM airport shuttles, the field lacks a holistic and systematic explorations to fully understand and optimize the system.

3. UAM airport shuttle framework

For the integration of Urban Aerial Mobility (UAM) services into the existing transportation ecosystem for airport shuttle operations, we present a comprehensive framework. This framework is designed to align with the characteristics and imperatives of commercial aviation users, grounded in research reports from governmental agencies, esteemed organizations, and reputable businesses (Hill et al., 2020; Greenfeld, 2019; EASA, 2021).

3.1. Vehicle and infrastructure

Electric Vertical Takeoff and Landing (eVTOL) aircraft are expected to become the primary choice for airport shuttle services over the next 5 to 10 years. In the evolving landscape of eVTOLs characterized by diverse propulsion configurations, the trend points to the preeminence of eVTOLs with superior power performance, particularly those featuring compound wing and tilt-rotor configurations. The incorporation of wings confers aerodynamic superiority, thereby facilitating higher cruising speeds and extended flight ranges. This is particularly crucial given the often considerable geographic separation of airports from urban centers, emphasizing the importance of time efficiency.

At the core of this framework are the shuttle vertiports, conceived as pivotal hubs within the UAM system. These vertiports are not confined to serving as mere parking facilities for eVTOLs; rather, they encompass multifaceted roles encompassing recharging, maintenance, and comprehensive upkeep. Converging at these shuttle vertiports, passengers are poised to initiate their journeys to airports or conclude their travels.

Concerns have been raised about integrating UAM operations, particularly on the side of airports. Strict regulations governing airspace around airports are in place globally to ensure aviation safety. Notable examples include the FAA's Part 107, UAS Facility Maps in the United States, EASA's European Drone geographical zones in Europe, and CAAC's interim regulations for unmanned aircraft flight management in China (UAS-Maps, 2023; EASA, 2023; CAAC, 2024). These regulations pose significant challenges to utilizing UAM for airport shuttle services: (1) eVTOLs typically operate between 150 m and 600 m to minimize ground interference, which conflicts with airport height restrictions, and (2) this limitation necessitates that passengers switch to ground transportation at a considerable distance from the airport, undermining the benefits of UAM.

Despite these challenges, there are concerted efforts underway to facilitate the integration of eVTOLs into existing airspace systems. Collaborative initiatives such as the FAA and Joby Aviation conducting safe operation trials at Dallas Fort Worth

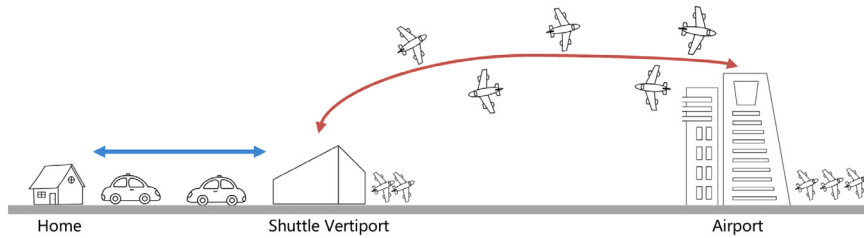


Fig. 2. Airport shuttle service using UAM.

International Airport and Love Field Airport ([NASA, 2023](#)), the UK's NATS simulating operations at Bristol, Envelope, and London City Airports ([NATS, 2023](#)), and Volocopter's flight trials in Pontoise ([Volocopter, 2022](#)), are pivotal. These efforts are geared towards merging Unmanned Aircraft System Traffic Management with Air Traffic Management, signaling a promising evolution towards more sophisticated air traffic management systems. Adjustments in policies and advancements in technology are paving the way for eVTOLs to become a viable option for airport shuttle services in the near future.

3.2. Airport shuttle service using UAM

The operational paradigm of this UAM system, as depicted in [Fig. 2](#), underscores a passenger-centric approach, informed by a diverse array of studies and reports ([McKinsey, 2022; Holden and Goel, 2016](#)). For passengers choosing airport shuttle services via UAM, the following procedures are envisaged:

For passengers heading to the airport:

- *Booking Service:* Passengers access a mobile booking platform to select their departure time and origin. The platform systematically identifies proximate available shuttle vertiports and provides passengers with pertinent flight-related information.
- *Travel to the Shuttle Vertiport:* Passengers undertake transit to the designated departure point, using their preferred modes of ground transportation, while maintaining real-time awareness of flight service statuses.
- *Boarding, Flying, and Landing:* This procedure involves efficient boarding at the shuttle vertiport, the smooth execution of flight operations, and the careful management of landing procedures.

For passengers leaving the airport:

- *Booking Service:* Analogously, passengers use a mobile application to specify their departure time and destination. The platform adeptly discerns suitable service routes for passengers.
- *Commencement of Flight Service:* Passengers embark upon the eVTOL at the airport, experiencing swift conveyance to the designated shuttle vertiport.
- *Travel to Destination:* After disembarking at the shuttle station, passengers proceed to ground transportation for the final segment of their journey to their ultimate destination, effectively concluding their entire service experience.

3.3. Modeling framework

Based on the service process described above, our modeling framework for UAM in the airport shuttle scenario emphasizes on several key settings aimed at ensuring the effectiveness and credibility of UAM operations:

- *Advance Reservation Orders:* To cater to the preferences of business air travelers who often book their flight tickets in advance, our model supports the option for passengers to reserve shuttle services well ahead of their departure. Once making a deal, operators are expected to commit fully to meeting these reservation requirements, except in cases of uncontrollable factors like adverse weather conditions, ensuring the credibility of UAM shuttle services.
- *Ad-Hoc Order Management:* Recognizing the occasional need for spontaneous airport shuttle services, such as flight rescheduling or departure delays, our model facilitates ad-hoc orders. To a certain degree, we permit demand for ad-hoc passengers to accommodate their immediate travel needs. For these ad-hoc orders, operators may consider implementing pricing strategies to encourage passengers to book in advance or set response limits to manage orders that exceed the system's capacity.
- *Comparative Evaluation of Transportation Modes:* We emphasize the importance of evaluating the quality of UAM services by comparing them to existing airport transfer modes, both in driving (e.g., taxis, online car-hailing, private vehicles) and public transit (e.g., subway, dedicated shuttle lines) transportation options. This evaluation ensures a comprehensive assessment of UAM services within the broader transportation landscape.
- *Service Time Composition:* Passenger time within UAM services encompasses four fundamental components: the first and last segments involving ground transportation to and from the airport, the interval devoted to security procedures and waiting, the duration of vertical takeoff and landing, and the actual in-flight time. To enhance efficiency, our approach promotes integration between UAM and commercial aviation transport, potentially allowing passengers to undergo a single security

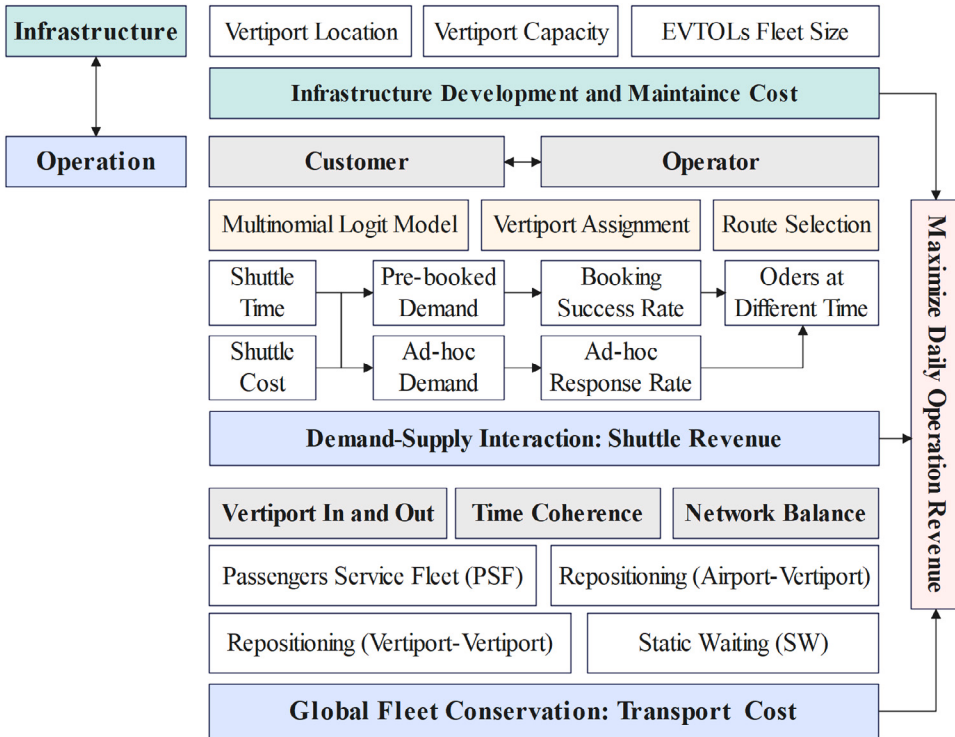


Fig. 3. UAM airport shuttle service planning model framework.

screening process. This streamlining of procedures aligns with high safety standards while reducing passenger time using UAM services.

While the aforementioned framework serve as an abstraction and simplification of UAM within airport shuttle service operations, it encapsulates fundamental elements, as dedicated in Fig. 3. These elements mirror the pivotal interactions between passengers and service providers. It is essential to note that not all reserved orders are guaranteed success, aligning with the realities observed in commercial flights and ride-sharing services, where reservations may not always be fulfilled. Nevertheless, it remains imperative to fully honor successfully reserved orders to uphold the service provider's credibility. The ad-hoc response mechanisms is designed to bolster the resilience of airport shuttle services through random responses. Ultimately, we aim to ensure credibility, reliability, and adaptability of UAM services in airport shuttle operations.

4. UAM airport shuttle planning model

The model's decision-making primarily involves vertiport selection and capacity design, the establishment of service routes, evaluation of UAM adoption, matching passengers with eVTOLs and vertiports, and overall vehicle balancing.

4.1. Vertiport construction

Vertiports, which serve as facilities for vertical takeoff and landing, are selected from a list of potential candidate sites \mathcal{N} . To represent whether a specific site is designated for vertiport construction, we introduce a binary variable denoted as x_i . Additionally, we introduce an integer variable H_i to determine the size of each shuttle vertiport i .

$\mathcal{N} \triangleq$ The set of candidates to establish vertical takeoff
and landing vertiports for airport shuttle services.

$$x_i = \begin{cases} 1, & \text{if a vertiport is constructed at candidate site } i \in \mathcal{N} \\ 0, & \text{otherwise} \end{cases}$$

$$H_i = \text{Capacity (to be determined) of shuttle vertiport, } i \in \mathcal{N}$$

Building vertiports within an urban environment involves significant construction and maintenance costs, making it a challenging task to create a dense network of vertiports within a city. Therefore, the number of vertiports must be restricted by a maximum

construction limit, denoted as \mathcal{R} in Eq. (1). Simultaneously, Eq. (2) ensures that capacity is allocated only when vertiport i is constructed and enforces a size constraint for each vertiport, limiting it to be less than C .

$$\sum_{i \in \mathcal{N}} x_i \leq \mathcal{R} \quad (1)$$

$$\mathcal{H}_i \leq C \cdot x_i \quad \forall i \in \mathcal{N} \quad (2)$$

4.2. Service route establishment

To monitor the system's dynamics across various intervals within the daily operational service time (OST), we partition the OST into M equidistant segments, each designated as a time window with a duration of T_0 (thus, $OST = M \cdot T_0$). The precise duration of each time window, T_0 , is determined based on the prevailing airport shuttle demand and the geographic coverage of the cities involved.

$OST \triangleq$ Operating Service Time. For example, from 6:00 AM to 10:00 PM,

the OST equals 16 h.

$\mathcal{T} \triangleq$ The indices set of all time windows within the OST , which ranges

from 1 to the maximum index t_{max}

$T_0 \triangleq$ The duration of each time window. The movement of eVTOLs for

passenger service or repositioning occur within each of these time windows.

$\mathcal{O} \triangleq$ All origins for passengers heading to the airport and all destinations

for passengers returning.

In our UAM system, the process of eVTOLs taking off is carefully regulated. The take-offs can exclusively occur at the very beginning of each designated time window (referred to as time window t). It is assumed that any demand specifying a desired takeoff time, such as the beginning of time window t , can only be met by eVTOLs departing precisely at the beginning of time window t , as opposed to time window $t + 1$ and beyond. Failure to adhere to this condition will lead to unfulfilled demand.

Any vertiport within the network can be utilized for serving demand originating from or destined to $o \in \mathcal{O}$. Here, \mathcal{O} represents all origins for passengers heading to the airport and all destinations for passengers returning. To assist operators in determining which shuttle vertiport $i \in \mathcal{N}$ to utilize to satisfy the passenger demand at a specific location $o \in \mathcal{O}$, we introduce the binary variable y_{oit}^+ and y_{oit}^- . Specifically, y_{oit}^+ signifies the service route heading towards the airport, while y_{oit}^- represents the service route departing from the airport.

$$y_{oit}^+(y_{oit}^-) = \begin{cases} 1, & \text{if a route heading to (departing from) the airport is established for vertiport} \\ & i \in \mathcal{N} \text{ at time } t \in \mathcal{T} \text{ to serve demand originating from (designating to) } o \in \mathcal{O} \\ 0, & \text{otherwise} \end{cases}$$

Eqs. (3) and (4) ensure that service routes exist only when vertiports are constructed. Simultaneously, Eqs. (5) and (6) guarantee that the demand at location $o \in \mathcal{O}$ at should be all completed by a single vertiport $i \in \mathcal{N}$.

$$y_{oit}^+ \leq x_i, \quad \forall o \in \mathcal{O} \quad \forall i \in \mathcal{N} \quad \forall t \in \mathcal{T} \quad (3)$$

$$y_{oit}^- \leq x_i, \quad \forall o \in \mathcal{O} \quad \forall i \in \mathcal{N} \quad \forall t \in \mathcal{T} \quad (4)$$

$$\sum_{i \in \mathcal{N}} y_{oit}^+ \leq 1 \quad \forall o \in \mathcal{O} \quad \forall t \in \mathcal{T} \quad (5)$$

$$\sum_{i \in \mathcal{N}} y_{oit}^- \leq 1 \quad \forall o \in \mathcal{O} \quad \forall t \in \mathcal{T} \quad (6)$$

Airport shuttle services connect passengers to various vertiports, resulting in varying costs for different service routes. Notably, time cost and monetary cost hold primary importance, especially for business air travelers. For passengers with origin or destination o planning to board eVTOL flights departing in time window t , we define their time costs using variables τ_{ot}^+ and τ_{ot}^- as described in Eqs. (7) and (8). This encompasses ground travel time to or from the vertiport (expressed as t_{oit}^{g+} and t_{oit}^{g-} , respectively), the average waiting time for security checks and passenger pooling at the vertiport (computed as $\frac{T_0}{2}$, where T_0 signifies the duration of each time window), the vertical ascent and descent time t_i^{add} , and the air flying time for passengers utilizing eVTOL t_i^f (assumed to be proportional to the straight-line distance). Simultaneously, Eqs. (9) and (10) elucidate the monetary costs λ_{ot}^+ and λ_{ot}^- of this journey, encompassing ground transportation fees p_{oit}^g and aerial travel costs p_i^f (where “+” and “-” denote the direction to and from the airport, respectively).

$$\tau_{ot}^+ = \sum_{i \in \mathcal{N}} (t_{oit}^{g+} + t_i^f + \frac{T_0}{2} + t^{add}) \cdot y_{oit}^+ \quad \forall o \in \mathcal{O} \quad \forall t \in \mathcal{T} \quad (7)$$

$$\tau_{ot}^- = \sum_{vi \in \mathcal{N}} (t_{oit}^{g-} + t_i^f + \frac{T_0}{2} + t^{add}) \cdot y_{oit}^- \quad \forall o \in \mathcal{O} \quad \forall t \in \mathcal{T} \quad (8)$$

$$\lambda_{ot}^+ = \sum_{vi \in \mathcal{N}} (p_{oit}^{g+} + p_i^f) \cdot y_{oit}^+ \quad \forall o \in \mathcal{O} \quad \forall t \in \mathcal{T} \quad (9)$$

$$\lambda_{ot}^- = \sum_{vi \in \mathcal{N}} (p_{oit}^{g-} + p_i^f) \cdot y_{oit}^- \quad \forall o \in \mathcal{O} \quad \forall t \in \mathcal{T} \quad (10)$$

4.3. UAM adoption evaluation

The UAM sector is still in the process of establishing large-scale operations, and as such, the precise extent of its demand remains unknown. In airport shuttle scenarios, UAM faces competition primarily from two traditional transportation modes: driving (e.g., taxis, online car-hailing, private vehicles) and public transit (e.g., subway, shuttle lines) transportation. Hence, it is crucial to estimate the volume of passengers who are willing to choose UAM services within the overall demand for airport transfers. To achieve this, we employ the Multinomial Logit Model (MNL), a well-recognized methodology widely used in fields such as economics and transportation (Bierlaire, 1998; Garrow, 2016). The MNL model is grounded in the principle of utility maximization, converting the utilities associated with various transportation modes or services into the probabilities of passenger selection. We utilize this model to estimate the demand for passengers inclined to use UAM for airport transfers.

Firstly, we determine the utilities associated with three modes of transport, focusing primarily on critical factors in travel decision-making, namely time and monetary cost. Eqs. (11), (12), and (13) define the utilities for driving (U_{ot}^d), public transit (U_{ot}^t), and UAM (U_{ot}^u), respectively. In these equations, V_{ot} represents the overall value of the journey, p_{ot}^d and p_{ot}^t denote the monetary cost of traditional driving and public transit modes, while t_{ot}^d and t_{ot}^t represent the time cost expending on these modes. The parameter b establishes the relationship between time and monetary cost, enabling us to measure the journey's average cost.

$$U_{ot}^d = V_{ot} - p_{ot}^d - b \cdot t_{ot}^d \quad \forall o \in \mathcal{O} \quad \forall t \in \mathcal{T} \quad (11)$$

$$U_{ot}^t = V_{ot} - p_{ot}^t - b \cdot t_{ot}^t \quad \forall o \in \mathcal{O} \quad \forall t \in \mathcal{T} \quad (12)$$

$$U_{ot}^u = V_{ot} - \lambda_{ot}^+ - b \cdot \tau_{ot} \quad \forall o \in \mathcal{O} \quad \forall t \in \mathcal{T} \quad (13)$$

With these utilities in place, we can calculate an upper limit on the response rate of UAM services by passengers using the MNL model. The UAM response rate α_{ot}^+ for a specific airport shuttle service route should remain below this upper limit, as defined in Eq. (14).

$\alpha_{ot}^+(\alpha_{ot}^-)$ = Response rate (for reserved orders) for a service route originating from (destining to) point o and taking off at given time window t .

To simplify this equation, we introduce the auxiliary parameter M_{ot}^+ (as outlined in Eq. (15)) to harmonize traditional driving and public transit transport modes. Additionally, the auxiliary variable γ_{ot}^+ (as described in Eq. (16)) represents the comprehensive cost of UAM. This simplification allows for a concise expression of the UAM response ratio (for reserved orders) from origin o to the airport, as shown in Eq. (17).

$$\alpha_{ot}^+ \leq \frac{e^{U_{ot}^{u+}}}{e^{U_{ot}^{u+}} + e^{U_{ot}^{d+}} + e^{U_{ot}^{t+}}} \quad \forall o \in \mathcal{O} \quad \forall t \in \mathcal{T} \quad (14)$$

$$M_{ot}^+ = e^{-p_{ot}^{d+} - b \cdot t_{ot}^{d+}} + e^{-p_{ot}^{t+} - b \cdot t_{ot}^{t+}} \quad \forall o \in \mathcal{O} \quad \forall t \in \mathcal{T} \quad (15)$$

$$\gamma_{ot}^+ = \lambda_{ot}^+ + b \cdot \tau_{ot}^+ \quad \forall o \in \mathcal{O} \quad \forall t \in \mathcal{T} \quad (16)$$

$$\alpha_{ot}^+ \leq \frac{1}{1 + M_{ot}^+ \cdot e^{\gamma_{ot}^+}} \quad \forall o \in \mathcal{O} \quad \forall t \in \mathcal{T} \quad (17)$$

We employ a similar methodology as in Eqs. (14) to (17) to introduce variables α_{ot}^- , M_{ot}^- and γ_{ot}^- , with the “-” symbol indicating the direction of service routes returning from the airport. This leads to Eqs. (18) to (21).

$$\alpha_{ot}^- \leq \frac{e^{U_{ot}^{u-}}}{e^{U_{ot}^{u-}} + e^{U_{ot}^{d-}} + e^{U_{ot}^{t-}}} \quad \forall o \in \mathcal{O} \quad \forall t \in \mathcal{T} \quad (18)$$

$$M_{ot}^- = e^{-p_{ot}^{d-} - b \cdot t_{ot}^{d-}} + e^{-p_{ot}^{t-} - b \cdot t_{ot}^{t-}} \quad \forall o \in \mathcal{O} \quad \forall t \in \mathcal{T} \quad (19)$$

$$\gamma_{ot}^- = \lambda_{ot}^- + b \cdot \tau_{ot}^- \quad \forall o \in \mathcal{O} \quad \forall t \in \mathcal{T} \quad (20)$$

$$\alpha_{ot}^- \leq \frac{1}{1 + M_{ot}^- \cdot e^{\gamma_{ot}^-}} \quad \forall o \in \mathcal{O} \quad \forall t \in \mathcal{T} \quad (21)$$

4.4. Demand response and flow allocation

4.4.1. Assigning passengers to vertiports

Passengers are assigned to appropriate vertiports for the commencement of their flight journeys. This assignment is facilitated by the allocation coefficient π_{oit}^+ , which allocates demand originating from point $o \in \mathcal{O}$ and scheduled for flight service during time

window $t \in \mathcal{T}$ to vertiport $i \in \mathcal{N}$. In Eq. (22), the left side represents the UAM response rate α_{ot}^+ (for reserved orders) from point $o \in \mathcal{O}$, while the right side signifies the allocation to different vertiports $i \in \mathcal{N}$.

In Eq. (23) (and also in Eq. (5)), we enforce that all reserved orders originating from the same point o within the same time window t should be directed to a single designated vertiport i . This constraint is essential for efficient passenger handling within each time window. Notably, passenger demand from different time windows retains flexibility and can be allocated to different vertiports. Furthermore, within a given time window t , passengers traveling from vertiport i to the airport may have various points of origin o . The summation in Eq. (24) calculates the total number of passengers ψ_{it}^+ that vertiport i must serve at that time window, considering that D_{ot}^+ represents the cumulative count of individuals requiring transportation from their specific origin o to the airport. Similarly, the allocation coefficients π_{oit}^- and the number of passengers returning from the airport ψ_{it}^- can be determined, as illustrated in Eqs. (25) through (27).

$$\alpha_{ot}^+ = \sum_{\forall i \in \mathcal{N}} \pi_{oit}^+ \quad \forall o \in \mathcal{O}, \forall t \in \mathcal{T} \quad (22)$$

$$\pi_{oit}^+ \leq y_{oit}^+ \quad \forall i \in \mathcal{N}, \forall t \in \mathcal{T}, \forall o \in \mathcal{O} \quad (23)$$

$$\psi_{it}^+ = \sum_{\forall o \in \mathcal{O}} D_{ot}^+ \cdot \pi_{oit}^+ \quad \forall i \in \mathcal{N}, \forall t \in \mathcal{T} \quad (24)$$

$$\alpha_{ot}^- = \sum_{\forall i \in \mathcal{N}} \pi_{oit}^- \quad \forall o \in \mathcal{O}, \forall t \in \mathcal{T} \quad (25)$$

$$\pi_{oit}^- \leq y_{oit}^- \quad \forall i \in \mathcal{N}, \forall t \in \mathcal{T}, \forall o \in \mathcal{O} \quad (26)$$

$$\psi_{it}^- = \sum_{\forall o \in \mathcal{O}} D_{ot}^- \cdot \pi_{oit}^- \quad \forall i \in \mathcal{N}, \forall t \in \mathcal{T} \quad (27)$$

Notably, Eqs. (17) and (21) pose nonlinear constraints. To linearize them, we introduce decision variables denoted as β_{otl}^+ and β_{otl}^- , employing a discretization method. In this context, A_l represents the discretized estimated values of the actual demand ratio α_{ot}^+ , where l encompasses the indices of values. Eqs. (28) to (33) outline the discretization and linearization process, with Eqs. (30) and (33) ensuring the uniqueness of the choice for α_{ot} . The symbols “+” and “-” indicate the direction of airport shuttle service in these Equations.

$\mathcal{L} \triangleq$ The set of indices for the discrete estimated values of α_{ot} .

$$\beta_{otl}^+ = \begin{cases} 1, & \text{if the discretized estimated value } A_l \text{ (with index } l\text{) for } \alpha_{ot}^+ \text{ is used} \\ 0, & \text{otherwise} \end{cases}$$

$$\beta_{otl}^- = \begin{cases} 1, & \text{if the discretized estimated value } A_l \text{ (with index } l\text{) for } \alpha_{ot}^- \text{ is used} \\ 0, & \text{otherwise} \end{cases}$$

$$\gamma_{ot}^+ \leq \sum_{\forall l \in \mathcal{L}} \ln\left(\frac{1 - A_l}{M_{ot}^+ \cdot A_l}\right) \cdot \beta_{otl}^+ \quad \forall o \in \mathcal{O}, \forall t \in \mathcal{T} \quad (28)$$

$$\sum_{\forall l \in \mathcal{L}} A_{l-1} \cdot \beta_{otl}^+ \leq \alpha_{ot}^+ \leq \sum_{\forall l \in \mathcal{L}} A_l \cdot \beta_{otl}^+ \quad \forall o \in \mathcal{O}, \forall t \in \mathcal{T} \quad (29)$$

$$\sum_{\forall l \in \mathcal{L}} \beta_{otl}^+ = 1 \quad \forall o \in \mathcal{O}, \forall t \in \mathcal{T} \quad (30)$$

$$\gamma_{ot}^- \leq \sum_{\forall l \in \mathcal{L}} \ln\left(\frac{1 - A_l}{M_{ot}^- \cdot A_l}\right) \cdot \beta_{otl}^- \quad \forall o \in \mathcal{O}, \forall t \in \mathcal{T} \quad (31)$$

$$\sum_{\forall l \in \mathcal{L}} A_{l-1} \cdot \beta_{otl}^- \leq \alpha_{ot}^- \leq \sum_{\forall l \in \mathcal{L}} A_l \cdot \beta_{otl}^- \quad \forall o \in \mathcal{O}, \forall t \in \mathcal{T} \quad (32)$$

$$\sum_{\forall l \in \mathcal{L}} \beta_{otl}^- = 1 \quad \forall o \in \mathcal{O}, \forall t \in \mathcal{T} \quad (33)$$

4.4.2. Assigning eVTOLs to vertiports

In the context of our UAM system, each eVTOL aircraft typically offers multiple seats, denoted as n , with a maximum passenger capacity of n individuals. As discussed in Section 3, our UAM system is able to serve both reserved and ad-hoc orders.

To determine the number of eVTOL flights required to transport reserved passengers to or from the airport for each shuttle vertiport i during time window t , we introduce integer variables U_{it}^+ and U_{it}^- , and Eqs. (34) and (35) provide the formulas for their calculation.

$$\frac{\psi_{it}^+}{n} \leq U_{it}^+ < \frac{\psi_{it}^+}{n} + 1 \quad \forall i \in \mathcal{N} \quad \forall t \in \mathcal{T} \quad (34)$$

$$\frac{\psi_{it}^-}{n} \leq U_{it}^- < \frac{\psi_{it}^-}{n} + 1 \quad \forall i \in \mathcal{N} \quad \forall t \in \mathcal{T} \quad (35)$$

Additionally, our model accounts for ad-hoc orders, which may arise due to factors like rescheduling, delays, or special circumstances. We represent these ad-hoc orders with e_{it}^+ and e_{it}^- . Eqs. (36) and (37) establish the lower bounds on the system's

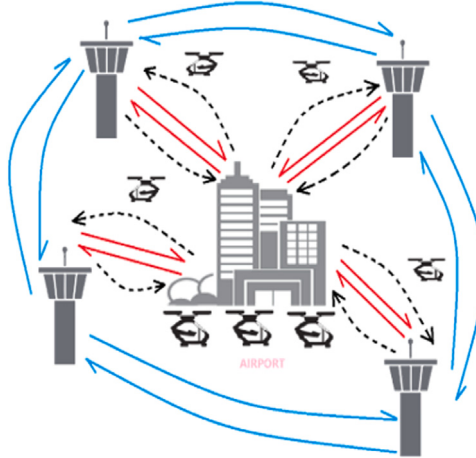


Fig. 4. Different eVTOLs' status in the network.

response (ρ_0) in handling these ad-hoc orders, highlighting the robustness of the UAM system. This parameter assists operators in determining the level of responsiveness based on the system's capacity. Subsequently, we calculate the number of ad-hoc orders that receive a successful response, using variables χ_{it}^+ for departures to the airport and χ_{it}^- for arrivals from the airport. Finally, Eqs. (38) and (39) convert these responded ad-hoc orders (χ_{it}^+ and χ_{it}^-) into the required number of eVTOL flights (D_{it}^+ and D_{it}^-).

$$\rho_0 \cdot \varepsilon_{it}^+ \leq \chi_{it}^+ \leq \varepsilon_{it}^+ \quad \forall i \in \mathcal{N} \quad \forall t \in \mathcal{T} \quad (36)$$

$$\rho_0 \cdot \varepsilon_{it}^- \leq \chi_{it}^- \leq \varepsilon_{it}^- \quad \forall i \in \mathcal{N} \quad \forall t \in \mathcal{T} \quad (37)$$

$$\frac{\chi_{it}^+}{n} \leq D_{it}^+ < \frac{\chi_{it}^+}{n} + 1 \quad \forall i \in \mathcal{N} \quad \forall t \in \mathcal{T} \quad (38)$$

$$\frac{\chi_{it}^-}{n} \leq D_{it}^- < \frac{\chi_{it}^-}{n} + 1 \quad \forall i \in \mathcal{N} \quad \forall t \in \mathcal{T} \quad (39)$$

4.5. Vehicle balancing

Within the context of our UAM system, eVTOLs operate within one of four primary operational states. These states are visually represented in Fig. 4 for clarity and reference:

- *Static waiting (SW)*: eVTOLs stationed at vertiports or the airport.
- *Passengers service fleet (PSF)*: eVTOLs engaged in fulfilling passenger orders.
- *Repositioning between two vertiports (RV)*: eVTOLs repositioning between different shuttle vertiports, without any passengers on board.
- *Repositioning between a vertiport and the airport (RVA)*: eVTOLs repositioning between a vertiport and the airport, without any passengers on board.

4.5.1. EVTOLs stationed at vertiports waiting for take-offs

In our UAM system, the process of eVTOLs taking off is carefully regulated. Regardless of whether these eVTOLs are designated for passenger service or repositioning, the take-offs can exclusively occur at the very beginning of each designated time window (referred to as time window t). During the time window immediately preceding t (referred to as time window $(t - 1)$), eVTOLs arriving at these designated locations are grouped and await their turn for take-off. This operational approach leads to a distinct operational pattern: the count of eVTOLs present at the shuttle vertiports or airports reaches its highest point at the conclusion of the preceding time window $(t - 1)$. Subsequently, this count temporarily declines due to the eVTOL take-offs that occur at the outset of the new time window t . To precisely model and quantify this operational pattern, we introduce two important integer variables W_{it} and E_t :

W_{it} = the count of eVTOLs stationed at vertiport $i \in \mathcal{N}$

at the start of time window $t \in \mathcal{T}$ (just before the new round of take-offs).

E_t = the count of eVTOLs stationed at the airport

at the start of time window $t \in \mathcal{T}$ (just before the new round of take-offs).

The values of W_{it} and E_t are subject to Eqs. (40) and (41) based on the capacity limitations of the shuttle vertiports and the airport.

$$W_{it} \leq \mathcal{H}_i \quad \forall i \in \mathcal{N} \quad \forall t \in \mathcal{T} \quad (40)$$

$$E_t \leq \Lambda \quad \forall t \in \mathcal{T} \quad (41)$$

4.5.2. eVTOLs departing from origin vertiports

For eVTOLs engaged in aerial transport, we introduce the following variables to represent the fleet quantities for PSF, RV, and RVA, respectively:

$P_{it}^+(P_{it}^-)$ = the count of PSF eVTOLs taked off at vertiport i to the airport
(taked off at airport to the vertiport i) at the start of time window t .

$L_{it}^+(L_{it}^-)$ = the count of RVA eVTOLs taked off at vertiport i to the airport
(taked off at airport to the vertiport i) at the start of time window t .

R_{ijt} = the count of RV eVTOLs taked off at vertiport i to vertiport j
at the start of time window t .

Here, the symbol “+” represents the direction of accessing the airport, while “−” represents the direction of leaving the airport. It is important to note that, due to the arrangement order of stations determined by i and j , there is no need for a “+” or “−” to distinguish R_{ijt} .

As previously mentioned, all eVTOLs used for passenger flights may originate from reservation and ad-hoc orders. Therefore, the total passengers service fleet (PSF) of shuttle vertiport i at time window t , denoted as P_{it}^+ and P_{it}^- , can be represented by Eqs. (42) and (43):

$$P_{it}^+ = U_{it}^+ + D_{it}^+ \quad \forall i \in \mathcal{N} \quad \forall t \in \mathcal{T} \quad (42)$$

$$P_{it}^- = U_{it}^- + D_{it}^- \quad \forall i \in \mathcal{N} \quad \forall t \in \mathcal{T} \quad (43)$$

4.5.3. eVTOLs arriving at destination vertiports

Given the take-off time of eVTOLs and the required flight duration of their journeys, we can calculate the arrival time of these eVTOLs at their destination vertiports. Recall that each time window has a duration of T_0 . We define the index $k \in \mathcal{K} = \{1, 2, \dots, k_{max}\}$, where k_{max} is obtained by dividing the flight duration required for a particular journey by the length of the time window T_0 and rounding up.

$$k_{max} = \lceil \frac{\text{flying duration}}{T_0} \rceil \quad (44)$$

$\mathcal{K} \triangleq$ The set of k range from 1 to k_{max} .

We introduce the parameter ζ_{ik} or ζ_{ijk} , which takes on the value of 1 only when a journey necessitates a flight across k time windows; otherwise, it is set to 0.

$$\zeta_{ik} = \begin{cases} 1, & \text{if the flying duration between shuttle vertiport } i \\ & \text{and the airport requests } k \text{ time windows} \\ 0, & \text{otherwise} \end{cases}$$

$$\zeta_{ijk} = \begin{cases} 1, & \text{if the flying duration between shuttle vertiport } i \\ & \text{and shuttle vertiport } j \text{ requests } k \text{ time windows} \\ 0, & \text{otherwise} \end{cases}$$

Consequently, we introduce Eqs. (45) and (46) to define P_{itk}^+ and P_{itk}^- for the PSF vehicles:

$$P_{itk}^+ = \zeta_{ik} \cdot P_{it}^+ \quad \forall i \in \mathcal{N} \quad \forall t \in \mathcal{T} \quad \forall k \in \mathcal{K} \quad (45)$$

$$P_{itk}^- = \zeta_{ik} \cdot P_{it}^- \quad \forall i \in \mathcal{N} \quad \forall t \in \mathcal{T} \quad \forall k \in \mathcal{K} \quad (46)$$

Similarly, Eqs. (47) and (48) introduce L_{itk}^+ and L_{itk}^- for the RVA vehicles:

$$L_{itk}^+ \leq \zeta_{ik} \cdot L_{it}^+ \quad \forall i \in \mathcal{N} \quad \forall t \in \mathcal{T} \quad \forall k \in \mathcal{K} \quad (47)$$

$$L_{itk}^- \leq \zeta_{ik} \cdot L_{it}^- \quad \forall i \in \mathcal{N} \quad \forall t \in \mathcal{T} \quad \forall k \in \mathcal{K} \quad (48)$$

Eq. (49) introduces R_{ijtk}^+ for the RV vehicles:

$$R_{ijtk} \leq \zeta_{ijk} \cdot R_{ijt} \quad \forall i \in \mathcal{N} \quad \forall t \in \mathcal{T} \quad \forall k \in \mathcal{K} \quad (49)$$

Following the above equations, we can interpret P_{itk}^+ as follows: If P_{itk}^+ equals zero, it means that the corresponding PSF vehicles taking off from vertiport i at the start of time window t will still be in transit and will not arrive at the airport before the start of

time window $(t + k)$. If P_{itk}^+ is greater than zero, it indicates that the corresponding PSF vehicles taking off from vertiport i at the start of time window t will arrive at the airport before the start of time window $(t + k)$ and will be available for future take-offs. Similar interpretations apply to other variables.

Notably, the choice of time window width is a critical operational parameter. Setting excessively narrow time windows can engender complexity in fleet management. In such instances, eVTOLs landing at specific moments may have originated from multiple preceding time windows, leading to intricate logistical complications. Conversely, overly wide scheduling time windows risk inducing idle eVTOLs post-completion of their assigned tasks. Hence, the establishment of judicious time windows, striking a balance between precision and flexibility, is essential.

4.5.4. Conservation of eVTOLs

Below equations offer a precise understanding of the eVTOL dynamics, aiding in the detailed analysis of eVTOL conservation within the system. Eq. (50) reveals the total eVTOL presence at vertiport i in readiness for take-offs as time window t begins. This count combines several key factors: the initial eVTOL count from the preceding time window $(t - 1)$, the net change in eVTOLs stemming from three distinct fleets during time window $(t - 1)$ — namely, the PSF vehicles represented by $\theta_{i,t-1}$ (as in Eq. (51)), the RV vehicles as captured by $\omega_{i,t-1}$ (from Eq. (52)), and the RVA vehicles denoted by $\eta_{i,t-1}$ (outlined in Eq. (53)). Each of these net changes factors in eVTOLs returning from airports or other shuttle vertiports and those departing from vertiport i during the respective time window.

$$W_{it} = W_{i,t-1} + \theta_{i,t-1} + \omega_{i,t-1} + \eta_{i,t-1} \quad \forall i \in \mathcal{N} \quad \forall t \in \mathcal{T}/\{1\} \quad (50)$$

$$\theta_{i,t-1} = \sum_{w=1}^{k_{max}} (P_{i,t-w,w}^- - P_{i,t-1,w}^+) \quad \forall i \in \mathcal{N} \quad \forall t \in \mathcal{T}/\{1\} \quad (51)$$

$$\omega_{i,t-1} = \sum_{j \neq i, j \in \mathcal{N}} \sum_{w=1}^{k_{max}} (R_{j,i,t-w,w} - R_{i,j,t-1,w}) \quad \forall i \in \mathcal{N} \quad \forall t \in \mathcal{T}/\{1\} \quad (52)$$

$$\eta_{i,t-1} = \sum_{w=1}^{k_{max}} (L_{i,t-w,w}^- - L_{i,t-1,w}^+) \quad \forall i \in \mathcal{N} \quad \forall t \in \mathcal{T}/\{1\} \quad (53)$$

Ensuring an adequate number of eVTOLs are stationed at each vertiport to meet dispatch requirements is crucial. Eq. (54) accomplishes this by ensuring the availability of a sufficient quantity of eVTOLs, denoted as W_{it} , for take-off from vertiport i at the start of time window t . This quantity includes the total number of RV, PSF, and RVA vehicles scheduled to depart from vertiport i at the start of time window t .

$$\sum_{j \neq i, j \in \mathcal{N}} \sum_{k \in \mathcal{K}} R_{ijtk} + \sum_{k \in \mathcal{K}} (P_{itk}^+ + L_{itk}^+) \leq W_{it} \quad \forall i \in \mathcal{N} \quad \forall t \in \mathcal{T} \quad (54)$$

At the end of each day's commercial operations, the system no longer requires the eVTOL fleet for passenger service. However, there may be a need for additional repositioning to restore eVTOL counts at each vertiport to their initial state at the beginning of the day to prepare for the next day's orders. Eq. (55) defines the tail repositioning variable w_i after daily operation service time (OST), which utilizes r_{ij} for RV repositioning from vertiport i to vertiport j and l_i^\pm for RVA repositioning between vertiport i and the airport. The “ \pm ” notation determines the direction of the fleet. In Eq. (56), we introduce the integer variable W_i^f to represent the number of eVTOLs at the final state at shuttle vertiport i . This variable is derived from the last eVTOL count ($W_{i,t_{max}}$), the last net change in the number of eVTOLs ($\theta_{i,t_{max}} + \omega_{i,t_{max}} + \eta_{i,t_{max}}$) and the tail repositioning process (w_i). Finally, Eq. (57) aims to reset any shuttle vertiport i to its initial state.

$$w_i = \sum_{j \neq i, j \in \mathcal{N}} r_{ij} - l_i^+ + l_i^- \quad \forall i \in \mathcal{N} \quad (55)$$

$$W_i^f = W_{i,t_{max}} + \theta_{i,t_{max}} + \omega_{i,t_{max}} + \eta_{i,t_{max}} + w_i \quad \forall i \in \mathcal{N} \quad (56)$$

$$W_i^f = W_{i,t=1} \quad \forall i \in \mathcal{N} \quad (57)$$

The same principle of maintaining a balanced eVTOL fleet applies to the airport as well. Eq. (58) calculates the quantity of eVTOLs stationed at the airport at the start of time window t . This calculation considers two components: the eVTOLs that were stationed at the start of the preceding time window $(t - 1)$ and the net change in eVTOL numbers during time window $(t - 1)$. The net change accounts for several factors, including the PSF vehicles arriving at and departing from the airport ($\sum_{i \in \mathcal{N}} \sum_{w=1}^{k_{max}} (P_{i,t-w,w}^+ - P_{i,t-1,w}^-)$) and the associated RVA vehicles ($\sum_{i \in \mathcal{N}} \eta_{i,t-1}$, as defined in Eq. (53)). Meanwhile, Eq. (59) ensures that there is a sufficient number of eVTOLs stationed at the airport to fulfill the dispatch requirements of PSF and RVA at the start of the time window t .

$$E_t = E_{t-1} + \sum_{i \in \mathcal{N}} \sum_{w=1}^{k_{max}} (P_{i,t-w,w}^+ - P_{i,t-1,w}^-) - \sum_{i \in \mathcal{N}} \eta_{i,t-1} \quad \forall t \in \mathcal{T}/\{1\} \quad (58)$$

$$\sum_{i \in \mathcal{N}} \sum_{k \in \mathcal{K}} (P_{itk}^- - L_{itk}^+) \leq E_t \quad \forall t \in \mathcal{T} \quad (59)$$

At the end of the OST, we address the final repositioning of eVTOLs at the airport by introducing variable e in Eq. (60), representing all RVA vehicles. Similar to Eq. (56), Eq. (61) derives the final count of eVTOLs at the airport, denoted as E^f . This

count is derived from the eVTOL count at the last time window $E_{t_{max}}$, and includes the following changes: changes resulting from PSF vehicles arriving at and departing from the airport ($\sum_{i \in \mathcal{N}} \sum_{w=1}^{k_{max}} (P_{i,t_{max}+1-w,w}^+ - P_{i,t_{max},w}^-)$) and RVA vehicles at the last time window, as well as the tail repositioning (e). Finally, Eq. (62) ensures that the airport returns to its initial state $E_{t=1}$ at the end.

$$e = \sum_{\forall i \in \mathcal{N}} (l_i^+ - l_i^-) \quad (60)$$

$$E^f = E_{t_{max}} + \sum_{i \in \mathcal{N}} \sum_{w=1}^{k_{max}} (P_{i,t_{max}+1-w,w}^+ - P_{i,t_{max},w}^-) - \sum_{i \in \mathcal{N}} \eta_{i,t_{max}} + e \quad (61)$$

$$E^f = E_{t=1} \quad (62)$$

In conclusion, we introduce integer variables M_t in Eq. (63), which aggregates the total counts of eVTOLs in all four states (PSF, RV, RVA, SW). The equation's right side consists of five components: the first two account for SW eVTOLs on the ground (E_t for airport and $\sum_{i \in \mathcal{N}} W_{it}$ for vertiports), while the next three represent PSF, RV, and RVA vehicles still in flight. Eq. (64) is specifically defined for $M_{t=1}$, encompassing the count of static waiting (SW) vehicles at the airport and shuttle vertiports, given that eVTOL transport has not yet begun before the start of the first time window. Finally, Eq. (65) ensures the overall conservation of eVTOLs within the system.

$$\begin{aligned} M_t &= E_t + \sum_{i \in \mathcal{N}} W_{it} + \sum_{i \in \mathcal{N}} \sum_{w=2}^{k_{max}} \sum_{x=1}^{w-1} (P_{i,x-w,w}^+ + P_{i,x-w,w}^-) \\ &+ \sum_{i \in \mathcal{N}} \sum_{w=2}^{k_{max}} \sum_{x=1}^{w-1} (L_{i,x-w,w}^+ + L_{i,x-w,w}^-) + \sum_{i,j \in \mathcal{N}} \sum_{w=2}^{k_{max}} \sum_{x=1}^{w-1} R_{i,j,x-w,w} \quad \forall t \in \mathcal{T}/\{1\} \end{aligned} \quad (63)$$

$$M_{t=1} = \sum_{i \in \mathcal{N}} W_{i,t=1} + E_{t=1} \quad (64)$$

$$M_{t-1} = M_t \quad \forall t \in \mathcal{T} \quad (65)$$

Similarly, we introduce M^f as the final global vehicle fleet size after daily operations in Eq. (66). Additionally, we establish the relationship between M^f and the initial fleet size $M_{t=1}$ using Eq. (67).

$$M^f = \sum_{i \in \mathcal{N}} W_i^f + E^f \quad (66)$$

$$M^f = M_{t=1} \quad (67)$$

4.6. Model objective

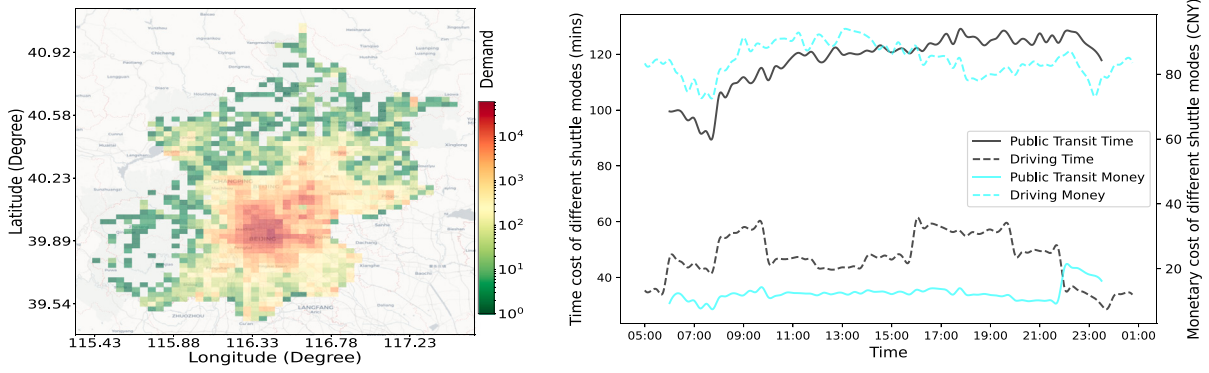
The viability of all operational details relies on the system's ability to consistently generate revenue. Therefore, we use Eq. (68), which aims to maximize the total profit (\mathcal{TP}), as the objective for our optimization model.

$$\begin{aligned} \max \quad \mathcal{TP} &= \sum_{i \in \mathcal{N}, t \in \mathcal{T}} \mathcal{E}_i ((U_{it}^+ + U_{it}^-) + \mu \cdot (D_{it}^+ + D_{it}^-)) \\ &- \sum_{i \in \mathcal{N}} (g_i \cdot x_i + m \cdot \mathcal{H}_i) - c^E \cdot M_{t=1} - m \cdot \Lambda \\ &- \sum_{i,j \in \mathcal{N}, t \in \mathcal{T}, k \in \mathcal{K}} c_{ij}^f R_{ijtk} - \sum_{i \in \mathcal{N}, t \in \mathcal{T}, k \in \mathcal{K}} c_i^f (L_{itk}^+ + L_{itk}^-) \end{aligned} \quad (68)$$

In the given equation, parameter \mathcal{E}_i stands for the total price of eVTOL flights between vertiport i and the airport, while μ represents the incentive coefficient for the operator to serve ad-hoc orders. Parameter g_i denotes the daily fundamental cost per vertiport, covering construction and maintenance expenses. Parameter c^E signifies the daily eVTOL operational cost, and parameter m denotes the cost of each eVTOL parking pad. Additionally, c_{ij}^f and c_i^f respectively indicate the RV and RVA repositioning costs. These parameters collectively form an equation used to calculate the pricing and cost considerations for eVTOL transportation and vertiport operations.

The entire problem is formulated as follows. This model is a mixed-integer linear programming (MILP) model and can be solved using the commercial solver (e.g., Gurobi):

- max \mathcal{TP} (Eq. (68)),
- s.t. Vertiport Construction: Eqs. (1)–(2),
Service Route Establishment: Eqs. (3)–(10),
UAM Adoption Evaluations (11)–(21),
Demand Response and Flow Allocation: Eqs. (22)–(39),
Vehicle Balancing: Eqs. (42)–(67)



(a) Transfer Demand of Beijing Capital Airport

(b) Time and Monetary Cost of Driving and Public Transit

Fig. 5. Airport transfer demand, time and monetary cost of existing modes.

5. Case study and results

5.1. Data and parameters

This section presents a case study on the Beijing Capital International Airport, chosen for three reasons: Firstly, passenger demand forecasts its potential. As a comprehensive hub, Beijing Capital International Airport handles numerous domestic and international flights daily, catering to many passengers. Secondly, there is a strong push for low-altitude passenger transport and innovative aviation development. For instance, the “Beijing Implementation Plan for Promoting Future Industry Innovation and Development (General Office of the People’s Government of Beijing Municipality, 2023)” and the “Beijing Action Plan for Promoting High-Quality Development of the Low-Altitude Economy (Beijing Municipal Bureau of Economy and Information Technology, 2024)” were introduced successively. Lastly, there are areas for improvement in existing airport shuttle services. In 2023, Beijing was ranked as the most congested city in China. Traffic congestion poses a significant risk for time-sensitive travelers who may miss flights, and the inconvenience of multiple public transportation transfers is a notable concern.

Given the nascent stage of UAM commercialization, our initial step involves examining the demand for airport shuttle services. We employ mobile signal data from China Unicom, strictly adhering to privacy and data protection protocols, to collect data on airport transfer demands in October 2020. However, 2020 was a year impacted by the COVID-19 pandemic. To estimate the typical airport transfer demand for Beijing under normal, non-pandemic conditions, we refer to Beijing Capital Airport’s report. This report provides insights into the percentage changes in shuttle demand during October 2020 compared to the same period in 2019. Additionally, we investigate China Unicom’s market share in Beijing, enabling us to arrive at a reliable estimation of the daily average airport transfer demand for Beijing Capital International Airport.

As illustrated in Fig. 5(a), the airport shuttle demands are aggregated into a grid system, with each grid having a longitude span of 0.045° and a latitude span of 0.027° . These grids collectively form a set of origins or destinations, denoted as \mathcal{O} . This set enables us to gather demand data, specifically D_{ot}^+ and D_{ot}^- , which represent demands to (denoted as “+”) and from (denoted as “-”) the airport within various time windows. The set of potential vertiport sites, denoted as \mathcal{N} , comprises the top 70 grids with high demand within set \mathcal{O} .

In our experiment, we use the demands D_{ot}^+ and D_{ot}^- as input data to estimate the number of passengers ψ_{it}^+ and ψ_{it}^- who successfully make advance bookings for UAM services. To simulate ad-hoc demand that may arise due to unforeseen circumstances like flight changes, we introduce a random uniform parameter h_{it}^\pm that ranges from 0 to 20%. The expressions $\epsilon_{it}^+ = \psi_{it}^+ \cdot h_{it}^+$ (and $\epsilon_{it}^- = \psi_{it}^- \cdot h_{it}^-$) represent the ad-hoc booking requests originating from location i to the airport or returning from the airport at the beginning of the time window t .

Within the context of airport shuttle scenarios, UAM primarily competes with two other modes of transportation: driving and public transit. To establish the fundamental parameters necessary for assessing passenger choice tendencies, we leverage web development services provided by Amap (Gaode Maps) to acquire data on the time and money associated with various transportation modes during different time windows. The resulting insights into time and monetary costs for driving and public transit are depicted in Fig. 5(b).

Fig. 6 shows the number of passenger flights taking off and landing at the Capital International Airport from October 29th to November 4th, 2023. Flights departing from the airport mainly occur between 6:00 AM and 10:00 PM, while those arriving are predominantly spread from 8:00 AM to 1:00 AM the next day. Since passengers must arrive at the airport in advance and spend time retrieving luggage upon departure, we set the UAM Operational Service Time (OST) from 5:00 AM to 1:00 AM the next day, totaling 20 h. Simultaneously, using 15 min as the duration T_0 for each time window, we thus obtain 80 equal-length time windows.

To facilitate the execution of our experiments and the subsequent evaluation of profits and costs, we introduce a set of fundamental parameters. These parameters are established based on insights derived from existing commercial reports, the current state of eVTOL technology development, and the research area’s consumption levels, dedicated in Appendix. Table 1 presents a summary of these parameters.

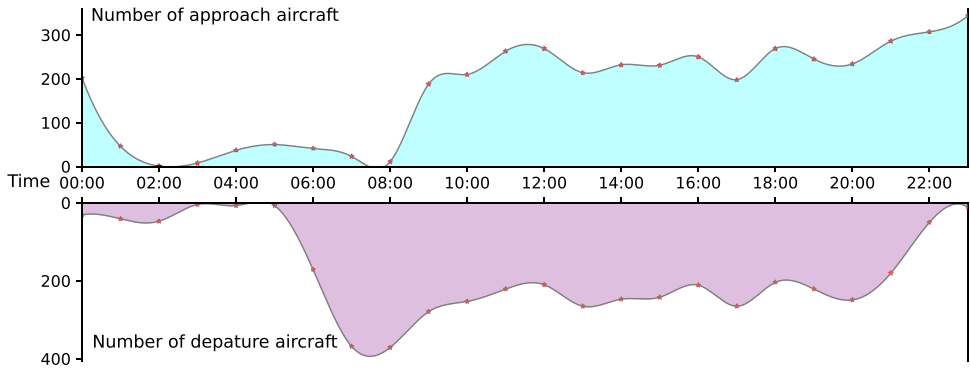


Fig. 6. Average flight arrival and departure numbers per hour at Beijing Capital International Airport from October 29th to November 4th, 2023.

Table 1
Parameters.

Symbol	Meaning	Units	Values
p_f^f	The price charged for each kilometer of eVTOL's flight	RMB	2.62
p_b^f	The cost incurred for each kilometer of flight repositioning	RMB	0.65
t^{add}	The duration taken for vertical takeoff and landing	min	5
v^f	The velocity at which the aircraft is flying	km/h	130/150/170/190
T_0	The length of a single time window in terms of time units	min	15
μ	The additional charge rate which is applied for dynamic orders	1	20%
ρ	The lowest level of response allowed for dynamic orders	1	80%
g_i	The fundamental daily cost associated with vertiport apron usage	RMB	191.8
m	The daily cost of each pad in the shuttle vertiports or airport	RMB	336.2
c^E	The daily cost incurred by each eVTOL vehicles	RMB	928.7
C	The highest number of pads available at vertiports	1	200
A	The highest number of pads available at the airport	1	500
b	The importance or value assigned to time, often related to decision-making or optimization processes.	1	2.5

5.2. System analysis

The proposed model is implemented in Python and executed on a PC configured with an Intel Core i9 CPU at 3.20 GHz and 128 GB of RAM. It achieves an optimal solution within 36.4 h, presenting a solution gap of 1.5%. This performance is considered acceptable, reflecting the model's design for non-immediate computation requirements. The model can finalize the calculations before the initiation of infrastructure construction, utilizing the available time effectively to ensure a thoroughly optimized solution for the development of infrastructure, including shuttle vertiports, landing pads, and eVTOLs, as well as their operational frameworks.

5.2.1. Network structure

The structural diagram, depicted in Fig. 7, offers a visual representation of the UAM airport shuttle service, comprising several pivotal components:

- Red circles: Vertiport locations, with varying circle sizes indicative of each vertiport capacity.
- Blue circle: Airport location, with the size indicative of the vertiport capacity of the airport.
- Red lines: Passenger service fleet (PSF), with line thickness representing the flow size.
- Green curves: Repositioning between vertiports and the airport (RVA), with line thickness representing the flow size and arrows showing the direction.
- Blue curves: Repositioning between different vertiports (RV), with line thickness representing the fleet size.

The network structure displays a radial, pyramid-shaped arrangement, with the airport serving as its central hub. Vertiports extend deep into urban areas, forming an extensive network that greatly improves connectivity between the city and the airport. Unlike rapid express lines such as the Capital Airport Line, the UAM system has strategically established a dense network of vertiports to reduce the reliance on ground transportation for the first and last-mile journeys to and from these vertiports.

Furthermore, the passenger service order flow between vertiports and the airport exhibits a strong unidirectional flow asymmetry, with a greater volume of RVA (Green Curve) traffic directed towards the airport, indicating the system's mobilization of vehicles to airports to accommodate a substantial number of passengers returning from the airports. However, this underscores one of the advantages of UAM — its flexibility, which arises from the smaller vehicle capacity. This flexibility enables high-frequency departures, reduces passenger waiting times, and achieves a high per-vehicle passenger load rate.

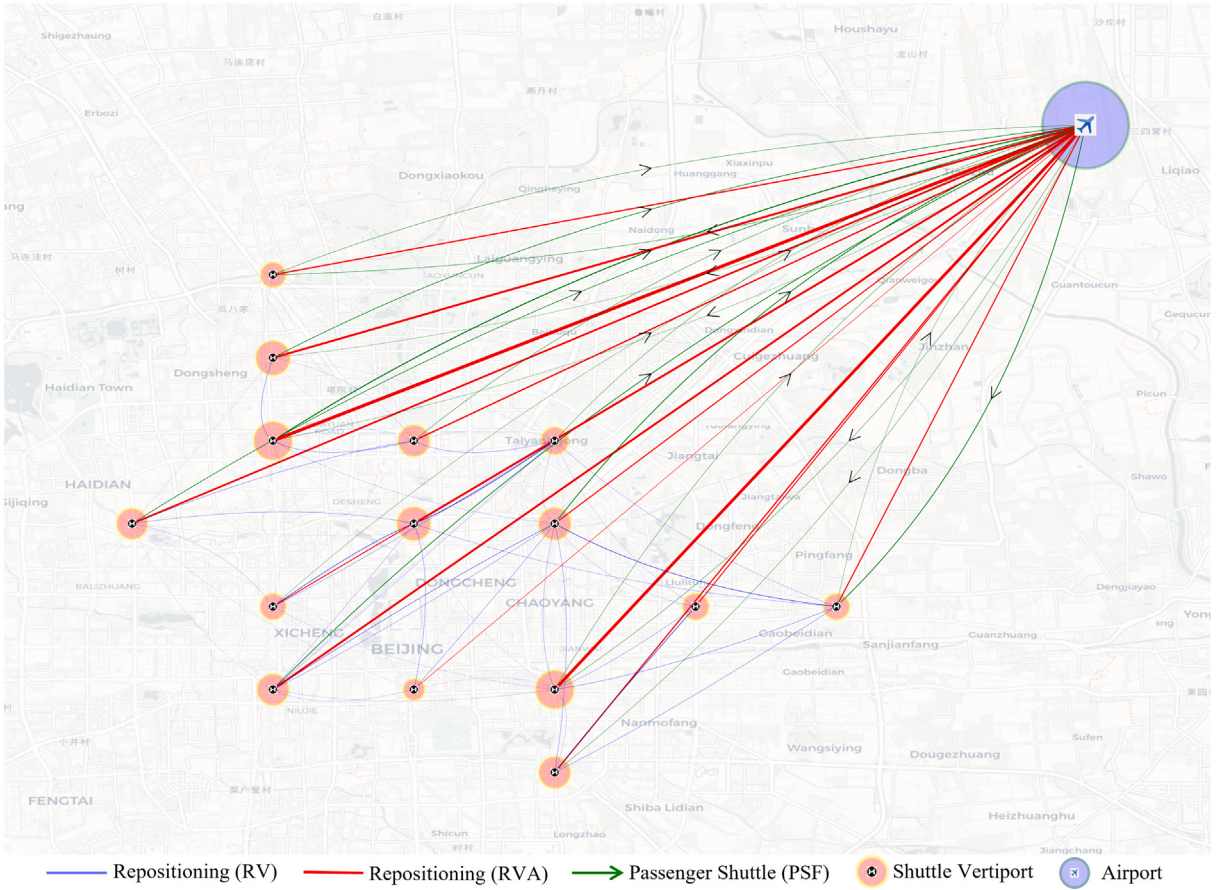


Fig. 7. UAM service network structure. (For interpretation of the references to color in this figure legend, the reader is referred to the web version of this article.)

In the context of the pyramidal-shaped connection network, our initial intuition was that vertiports located near the airport would exhibit a higher frequency of RVA (Green Curve) activity. Conversely, those situated farther from the airport were expected to primarily engage in frequent RV (Blue Curve) exchanges with neighboring sites, using the “vehicle transfer” method to significantly reduce the time and monetary costs associated with flight rebalancing. However, upon closer examination in Fig. 7, a different pattern emerges: eVTOLs used for RV purposes are consistently and densely commuting between various vertiports, and RVA activity is present regardless of a vertiport’s proximity to the airport.

The underlying causes of this observed phenomenon are intricate. A plausible explanation can be proposed: Each eVTOL has the potential to generate revenue from up to three passengers, resulting in per-kilometer equivalent revenue that surpasses the cost required for per-kilometer repositioning. As a result, it is financially advantageous to directly dispatch vehicles from the airport to any vertiport. On the other hand, the cost associated with each helipad, denoted as m , remains constant regardless of whether it is located at a vertiport or the airport. The adoption of a “vehicle transfer” approach for dispatch would imply the need for more helipads at these transfer-centric sites.

5.2.2. UAM welfare analysis

Fig. 8 provides a comprehensive comparison of time and monetary costs for three modes of transportation: driving, public transit, and UAM. Among these modes, UAM stands out as the swiftest option, boasting an average travel time of merely 46.5 min. This represents a substantial improvement over driving, which consumes an average of 64.9 min, and public transit, necessitating an average of 113 min. UAM delivers significant time savings, reducing travel times by 28.4% compared to driving and a remarkable 58.8% compared to public transit. These time savings enhance passenger mobility between the city and the airport. In terms of monetary costs, UAM services are competitive with driving fares, averaging around 90.3 RMB compared to 91.3 RMB for driving, but notably higher than the 18.2 RMB of public transit. Despite UAM having a higher per-kilometer charge than driving, its utilization of more direct flight routes results in shorter travel distances, ultimately leading to comparable monetary costs with the driving mode.

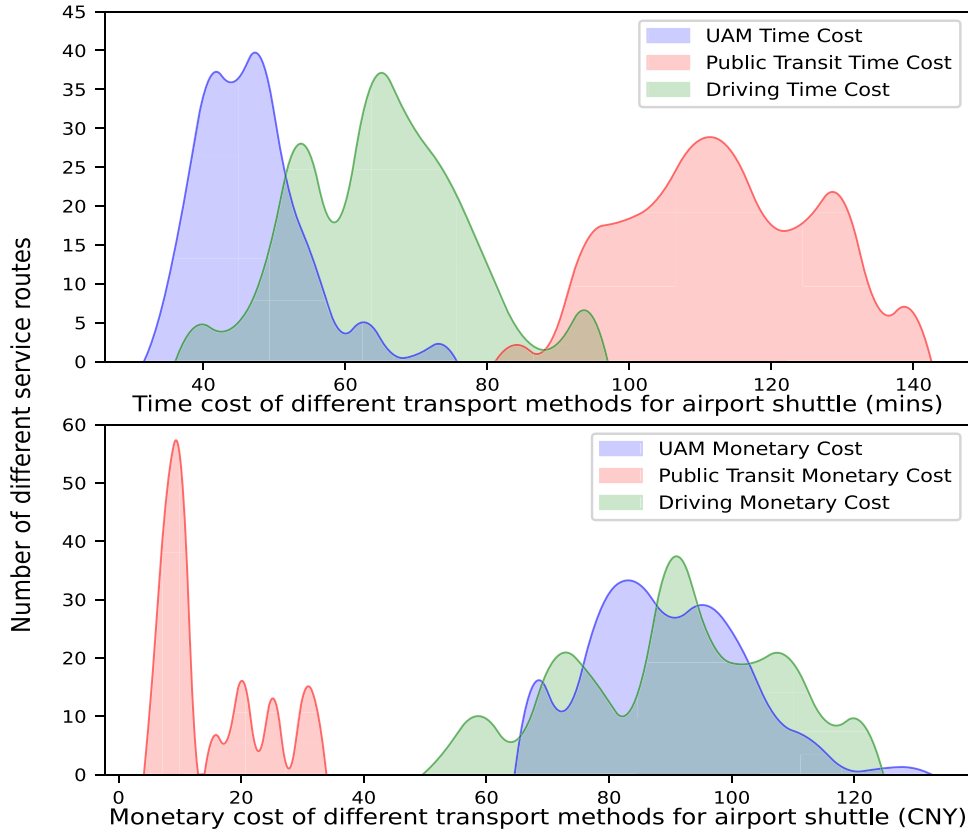


Fig. 8. UAM service routes' average time and monetary cost compared to driving and public transit.

Figs. 9(a) and 9(b) offer a detailed breakdown of the time and monetary cost associated with using UAM for various airport transfer distances. Notably, in average, 48.6% of the total travel time is devoted to first and last-mile ground transportation, underscoring a substantial portion of travel time spent on ground public transit. An additional 23.7% is allocated to waiting for takeoff and vertical landing processes, leaving only 27.7% of the time for actual in-air flight. This highlights the potential to shift some of this traffic to three-dimensional airspace or enhance ground transportation will further amplify the advantages of UAM. Moreover, the integration of UAM into airport shuttle services can streamline various tasks, including airport security checks. UAM and traditional aviation adhere to the same safety standards, enabling a seamless collaborative model. This integrated approach eliminates the need for passengers to arrive at the airport well in advance, resulting in significant time savings.

Regarding monetary costs, approximately 69.7% of expenses can be attributed to the flight phase, emphasizing the substantial fees associated with eVTOL services. For distances below 23 km, UAM incurs higher costs compared to driving. Conversely, for longer airport transfer distances, driving becomes more expensive. This cost distribution is due to the fact that longer routes often necessitate ground transportation through congested urban areas, leading to a substantial increase in associated costs. In contrast, UAM charges primarily depend on the direct flight distance and are unaffected by ground congestion.

In summary, the analysis affirms the viability of UAM within airport transfer services from a welfare perspective. UAM combines the reliability of public transit with the flexibility, privacy, and speed associated with driving. This mode of transport is particularly well-suited for passengers willing to pay premium fares, offering them a dependable and expedited travel experience between the airport and congested urban areas. UAM is poised to secure a significant market share, effectively competing with traditional driving modes such as taxis and ride-sharing services. Moreover, UAM's primary strength lies in its ability to bypass traffic congestion. Any initiatives aimed at reducing ground transportation time, such as improvements to ground traffic or the provision of long-distance shuttle services, will further enhance the advantages offered by UAM.

5.2.3. Demand and response

The integration of UAM into airport shuttle services combines both reserved and ad-hoc orders. Throughout daily operations, passengers and operators continually adapt to each other's needs. Fig. 10 depicts the demand and response patterns throughout the day, with time windows, each representing 15 min, plotted on the x-axis. Notably, the majority of shuttle service requests occur between 7:00 AM and 10:00 PM. During this period, operators efficiently respond, maintaining a strong response rate for reserved orders, averaging 0.948. Additionally, the vehicle utilization rate for passenger transportation achieves an average of 0.738.

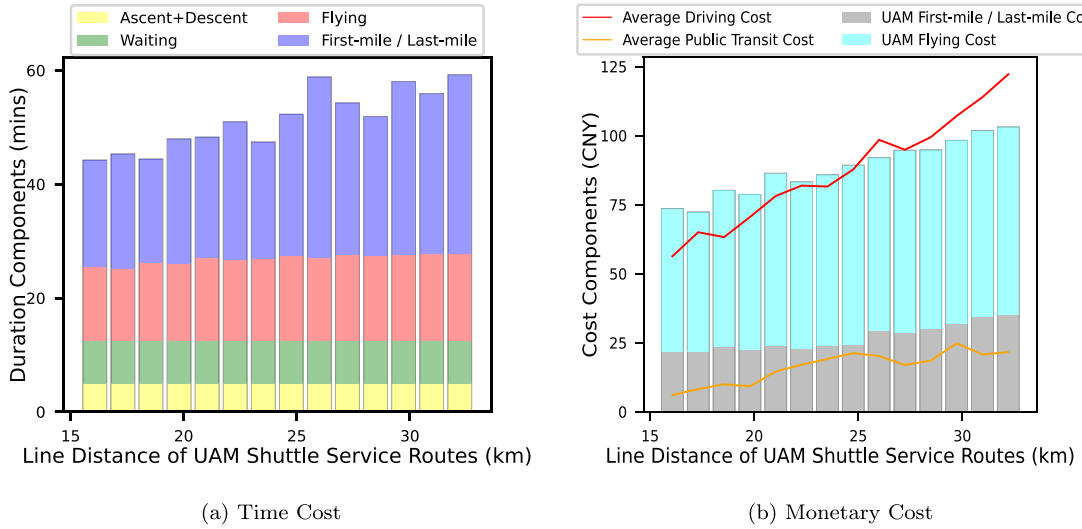


Fig. 9. Time and monetary cost analysis across various airport transfer distances (Euclidean Distance from origin or destination to the airport).

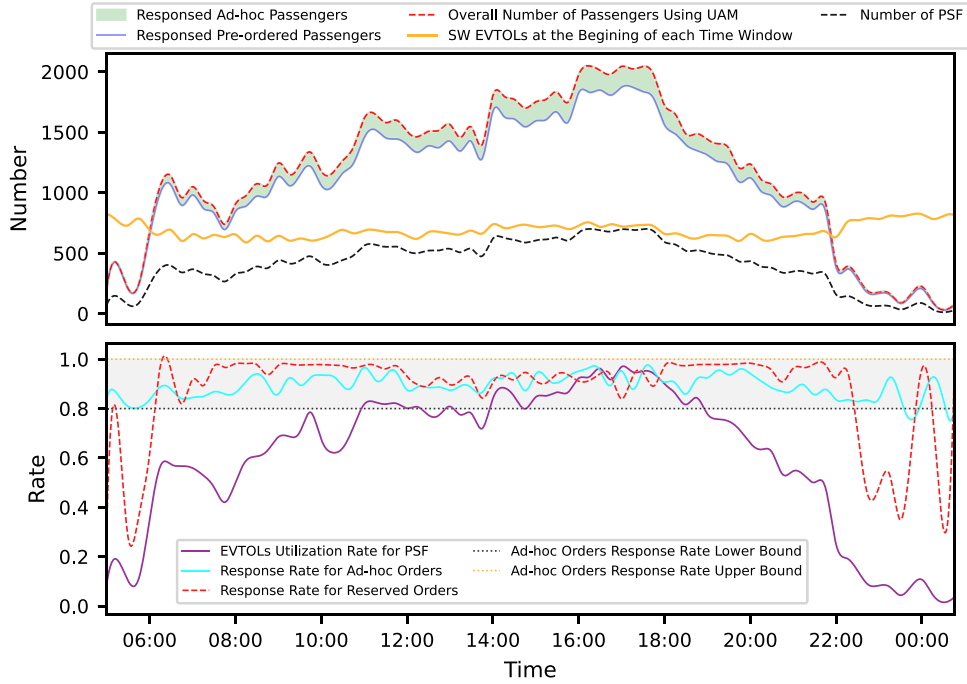


Fig. 10. Demand, response and vehicle utilization.

However, the variability in ad-hoc orders introduces an element of uncertainty that may disrupt the equilibrium of the UAM system, leading to a slightly lower average response rate of 0.907 compared to reserved orders.

The peak in shuttle demand is observed from 3:00 PM to 6:00 PM, influenced by several factors, including the arrival of morning flights, departures of afternoon flights, and the evening commute of airport staff. Consequently, demand reaches its highest point during these hours, and vehicle utilization rates escalate to 0.818, reaching their peak as well. Notably, there is a momentary dip in the response rate for reserved orders during demand peaks, like the operation time around 17:00. This phenomenon is attributed to the system's need to control the escalation in the number of vehicles operating within the system. Adding excessive vehicles during peak demand periods would lead to resource wastage and result in additional costs for both vehicles and vertiports. Hence, the system maintains control by reducing the response rate of reserved orders during these high-demand hours.

An interesting phenomenon occurs during the initial and final two hours of daily operation, spanning from 5:00 AM to 7:00 AM and from 11:00 PM to 1:00 AM. There is considerable and fluctuating variation in the response rate for reserved orders, which

Table 2
Response rate of reserved orders in different time.

Time	Vertiport to airport	Airport to vertiport
Morning	0.642	0.955
Night	0.897	0.548

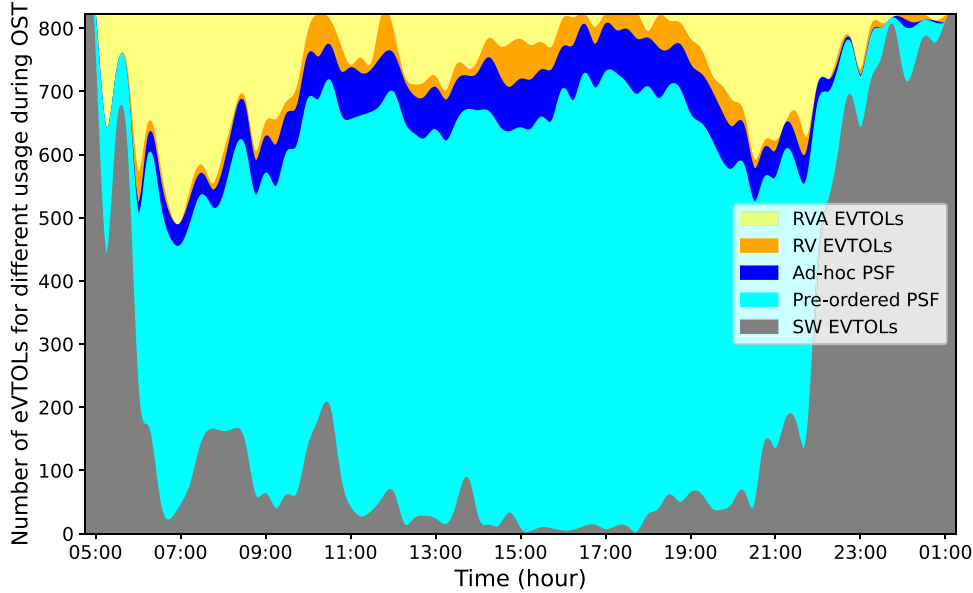


Fig. 11. EVTOLs' usage for different purpose (RVA EVTOLs, RV EVTOLs, PSF for reserved (Pre-ordered) orders, PSF for Ad-hoc Orders, SW EVTOLs).

tends to remain relatively low. This trend primarily stems from the unidirectional nature of demand at these times, with passengers predominantly commuting to the airport in the morning and returning in the evening. The system's response is to deliberately lower the response rate for reserved orders during these specific times as a strategy to manage and control the elevated operational costs. Supporting this interpretation, [Table 2](#) provides additional evidence by displaying the response rate for reserved orders during these early morning and evening hours for both directions—heading to the airport and returning from the airport.

5.2.4. Vehicle usage

The system comprises four vehicle status, as detailed in Section 4: passenger service (PSF, for serving reserved and ad-hoc orders), repositioning between vertiports (RV), repositioning between vertiport and airport (RVA), and static waiting (SW). [Fig. 11](#) visually illustrates the fluctuations in vehicle usage.

In [Fig. 11](#), there is a noticeable decrease in idle vehicles during the primary service hours, with a higher concentration of idle vehicles in the early morning and late evening hours. Meanwhile, the majority of repositioning activities occur between the airport and vertiports in the early or late stages of each day, indicating an imbalance in bi-directional airport transfer demand. Additionally, an uptick in repositioning activities between vertiports is observed when the system experiences higher order volumes. This phenomenon can be attributed to two primary factors. Firstly, only short-distance RV processes can be swiftly completed within 0 to 30 min, ensuring a sufficient supply of eVTOLs during rush hours. Secondly, the system's equilibrium improves with higher demand, reducing the number of vehicles required for repositioning.

Additionally, daily vehicle usage patterns at each vertiport during operational hours can be observed. [Fig. 12](#) illustrates vehicle utilization at fifteen different vertiports. In the morning, a significant number of vehicles are repositioned from the airport to these vertiports, such that more available vehicles can serve commuters or passengers catching early morning flights. Later in the day, there is a notable increase in repositioning activities from the vertiports to the airport, specifically catering to returning passengers. These fluctuations in repositioning between shuttle vertiports and the airport (RVA) reflect the real-time dynamics of airport transfer demand and indicate the system's imbalances during these time periods. However, such activities are relatively less common during the mid-operation hours. This imbalance during that period is primarily addressed by lower-cost repositioning between vertiports (RV).

An interesting observation emerges during the mid-operation hours: the peak of PSF vehicle flow towards the airport aligns with the low point of PSF vehicle flow back from the airport, and vice versa. This scheduling phenomenon can be attributed to the extensive and interconnected vertiport network. This network enables residents from various city areas to choose from multiple

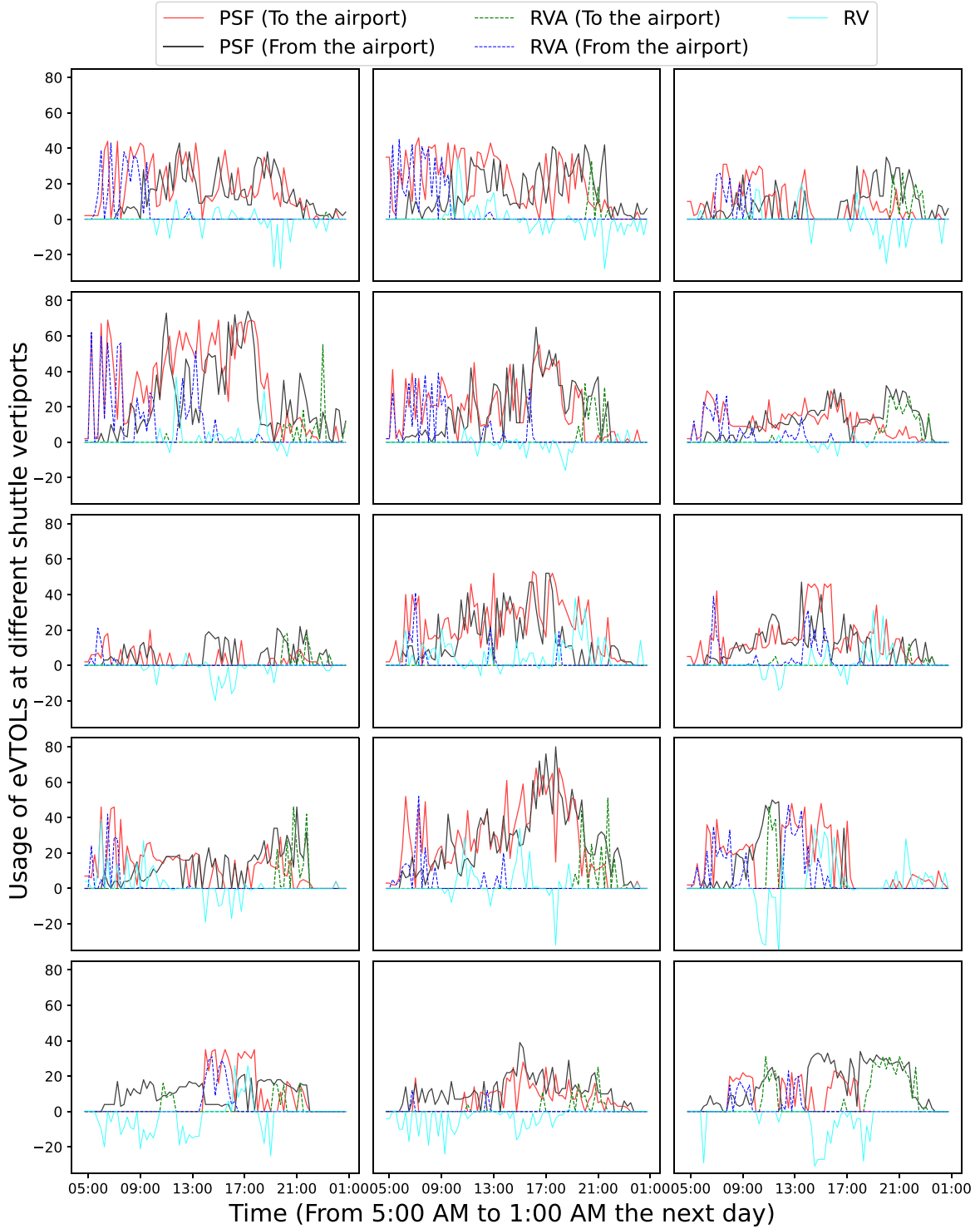


Fig. 12. The usage of eVTOLs in each vertiport.

vertiports for their journeys to and from the airport, resulting in minimal fluctuations in both travel time and costs. Consequently, when a vertiport predominantly serves departures during one time window, it subsequently receives incoming vehicles from the airport during the following time window, and vice versa. This observation underscores the importance of centralized operational management in the UAM system, where passengers follow the system's guidance for their eVTOL boarding shuttle service.

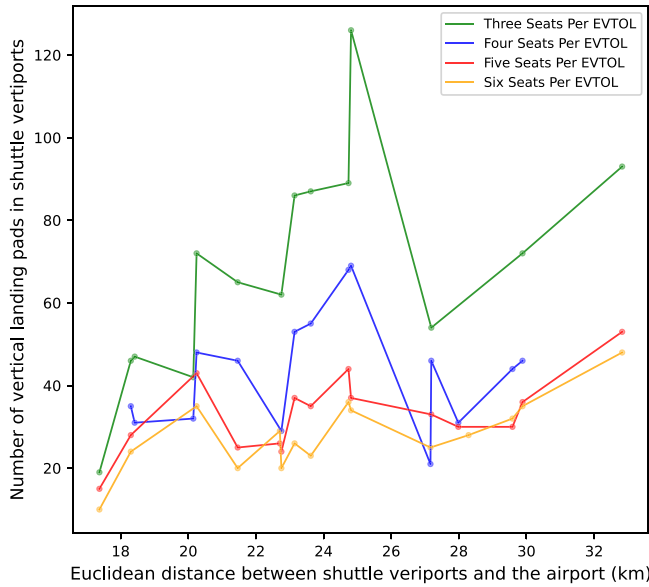


Fig. 13. Impact of eVTOL capacity on network structure.

Table 3
Impact of eVTOL capacity on system operations.

Capacity	Profit	Fleet	Passengers	Money	Time	Flights	RV+RVA	PSF	SW
3 passengers	¥4554k	1260	85,797	64.4	14.8	60,416	14.4%	59.4%	26.2%
4 passengers	¥5163k	822	85,522	63.8	14.7	40,361	14.5%	57.0%	28.5%
5 passengers	¥5934k	733	86,901	67.16	15.25	32,076	13.9%	53.4%	32.7%
6 passengers	¥6212k	625	86,534	67.21	15.26	26,017	13.1%	50.9%	36.0%

5.3. Sensitive analysis

5.3.1. eVTOL capacity

Passenger capacity in eVTOL aircraft varies due to their distinct propulsion systems. Currently, with the exception of the Lilium Jet, which can accommodate up to seven passengers, most eVTOLs typically have a capacity ranging from 3 to 6 passengers. Therefore, we conduct an analysis to comprehend the impact of these varying passenger capacities on airport shuttle systems.

Fig. 13 illustrates how vertiport sizes change in relation to their distance from the airport, taking into account different vehicle capacities. In terms of network layout, vertiports can be broadly categorized into three groups: short-range, medium-range, and long-range. When the passenger capacity is set at 3, the system can only generate additional profits for a maximum of 3 passengers per vehicle. Consequently, large-scale vertiports are strategically placed in the city center to serve medium-distance airport transfer passengers efficiently, accommodating passengers from all parts of the city. As the passenger capacity increases from 3 to 4, there are small adjustments in the network structure — the overall size of the vertiports decreases due to the increased passenger capacity per eVTOL. However, a noteworthy transformation occurs within the network structure with higher passenger capacities (e.g., 5 to 6 individuals). On one hand, the disparities in scale among vertiports of the three levels decrease, resulting in more balanced development. Simultaneously, their overall size is smaller compared to systems using eVTOLs with 3 or 4 passengers. On the other hand, super vertiports with peak capacity shifts towards the long-range category due to substantial revenue opportunities for high-capacity vehicles. As a result, long-range vertiports significantly expand their capacity to accommodate extensive airport transfer demand from areas far beyond the airport.

Table 3 offers a detailed exploration of how eVTOL capacity influences the system operations. The increase in vehicle capacity leads to higher profits (in thousands of RMB). Transitioning from a 4-passenger to a 5-passenger configuration results in significant gains due to network-related adjustments. Although the increase in the total number of daily served passengers remain marginal, the system's eVTOL fleet size decreases. From the passenger's perspective, increased passenger capacities result in higher expenses and longer flight durations. This implies a system preference for accommodating long-range shuttle requests, highlighting that larger eVTOLs are more suitable for medium to long-distance travel. Also, from a vehicle standpoint, daily flight frequencies gradually decrease. Additionally, large-capacity eVTOLs enhance system balance, which can be observed from the reducing usage rate of empty repositioning (RV+RVA). However, high capacity also leads to decreased vehicle utilization rates (PSF) and an increased proportion of daily idle waiting (SW).

When considering commercial implementation in the airport shuttle scenario, the utilization of high-capacity eVTOLs offers several advantages to the UAM system. Firstly, vertiport sizes remain relatively uniform, eliminating the need for large airport

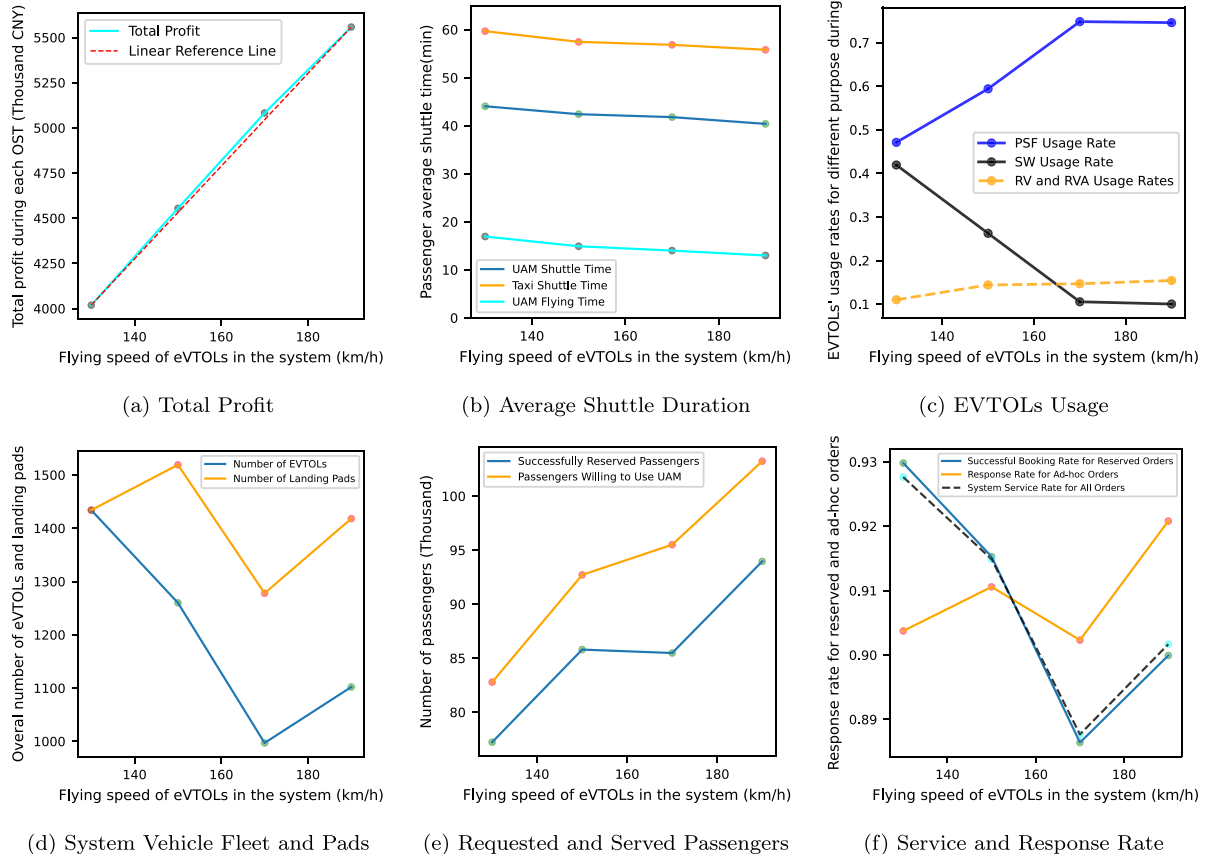


Fig. 14. Impact of EVTOL flight speed on system operations.

constructions in city centers, thereby enhancing infrastructure feasibility. Secondly, high-capacity eVTOLs reduce the overall fleet size with slight variation in passenger service, reducing airspace congestion and improving operational viability. Moreover, additional repositioning is reduced, enhancing overall system balance and resilience in response to fluctuating demands. Furthermore, high-capacity vehicles contribute additional revenue and economic viability to the system. Finally, they provide more idle waiting time for eVTOL charging, maintenance, and safety checks. However, the use of high-capacity vehicles steers UAM in the airport shuttle sector towards a more scheduled service model at the expense of flexibility and passenger privacy.

5.3.2. Flying speed

Flight speed is a critical performance metric in the evaluation of eVTOL systems. Publicly available specifications for eVTOL vehicles typically indicate a speed range of 100 km/h to 250 km/h. To investigate the implications of flight speed, our experiments are conducted at four specific settings within the range, specifically: 130 km/h, 150 km/h, 170 km/h, and 190 km/h. Fig. 14 presents the results of these experiments. Overall, an increase in flight speed results in almost linear growth in daily profitability while the system continues to exhibit high resilience, maintaining a response rate of approximately 91% for ad-hoc orders.

When the flight speed increases from 130 km/h to 150 km/h in the UAM system, it reduces the average travel time for passengers commuting between vertiports and airports. This heightened velocity leads to a more efficient transportation system, characterized by increased vehicle activity during operational service time (OST). This includes a significant rise in passenger service fleet (PSF) utilization rate, more repositioning processes (RV, RVA), and fewer eVTOLs waiting in static (SW). This efficiency also leads to a reduction in the fleet size of eVTOLs in the system. At a speed of 130 km/h, the vertiport size matches the eVTOL fleet size, indicating no need for surplus pads. However, at 150 km/h, due to higher eVTOL movement frequency, a smaller fleet requires more helipads to meet demand. Additionally, higher speeds attract more passengers to use the service, extending shuttle services to more passengers traveling between urban areas and airports. However, the overall service rate and successful booking rate of reserved orders slightly decline slightly because the UAM system prioritizes fulfilling demands that benefit its overall operation and profitability.

As flight speed increases from 150 km/h to 170 km/h, there is a notable intensification in the system's activity. Shorter flight times encourage more individuals to consider using UAM. However, in contrast to the previous speed increase, when faced with a

surge in service requests, the system experiences a slight decrease in the number of passengers successfully served, accompanied by a rapid decline in the overall service response rate. This outcome can be plausibly attributed to the enhanced operational flexibility facilitated by faster flight speeds. Almost all flight fleets (including PSF, RV, and RVA) are able to complete their actions within a single time window. This leads to a more efficient utilization of eVTOLs for transportation purposes, reducing the waiting time for subsequent use (SW). Consequently, it results in a notable reduction in both the fleet size and the number of required take-off and landing pads. This, in turn, leads to substantial cost savings and a significant boost in the system's overall revenue.

As flight speed is further increased to 190 km/h, an enhanced willingness to utilize UAM becomes evident, primarily owing to its high-speed advantage. Simultaneously, the utilization rate of PSF remains constant, signifying that the vehicles within the system are fully deployed, reaching their operational capacity limit. Under these circumstances, operators can only augment service capacity and reap greater profits through investments in additional eVTOLs and helipad facilities, leading to an increase in the total number of individuals served and an enhancement in the response rate.

6. Conclusion

This study investigates the potential implementation of Urban Air Mobility (UAM) for airport shuttle services and proposes a comprehensive strategy that integrates strategic decision-making and operational tactics. The research covers critical aspects, including UAM demand estimation, vertiport selection, vertiport capacity design, route optimization, service responsiveness, and scheduling.

Through a case study at Beijing Capital International Airport, our findings reveal the potential of UAM, demonstrating a significant 28.4% reduction in passenger travel time while maintaining monetary cost comparable to traditional ground transportation alternatives. Opportunities for improving UAM's time-saving capabilities, particularly through ground transportation optimization and collaboration with commercial aviation, have been identified.

The study highlights the reliability of the UAM system, with a 94.8% response rate for reserved orders and a 90.7% response rate for ad-hoc orders. Also, we uncover the repositioning strategy, which contributes to the system's resilience. Long-distance repositioning between the airport and vertiports is most pronounced during peak morning and evening hours, while cost-saving repositioning between nearby vertiports primarily takes place during mid-operation hours. Furthermore, the distribution of UAM vertiports and scheduling strategies have been outlined, highlighting their roles in facilitating passenger transitions and operational efficiency.

Finally, our sensitivity analyses pertaining to passenger capacity and eVTOL flight speed provides insights. The findings indicate that larger-capacity vehicles accommodating 5 to 6 passengers offer potential benefits in terms of infrastructure development, operational scheduling, and energy replenishment, despite potential trade-offs in privacy and flexibility. Additionally, increased flight speed exhibits a nearly linear correlation with revenue growth, indicating a promising avenue for future UAM initiatives.

This study encourages further research efforts to expand the scope, including investigations into UAM applications in diverse cities, especially those with multiple airports. Exploring adaptable scheduling approaches for both reserved and ad-hoc orders is vital for accommodating real-world operational scenarios. Additionally, a comprehensive examination of actual flight routes for airport shuttle services, considering non-idealized conditions, is essential for practical implementation. These research directions will contribute to the continued advancement of UAM as a transformative transportation solution.

CRediT authorship contribution statement

Di Lv: Writing – original draft, Methodology. **Wei Zhang:** Writing – original draft, Methodology. **Kai Wang:** Writing – review & editing, Methodology. **Han Hao:** Writing – review & editing, Validation. **Ying Yang:** Writing – review & editing, Validation.

Data availability

Data will be made available on request.

Acknowledgment

This work was supported by the National Natural Science Foundation of China (grant 72322002).

Appendix

UAM is at an early stage which lacks universally accepted parameters. Meanwhile, regions always have different standards. Therefore, we made some estimations according to the development of UAM and the living standard in Beijing:

1. Daily Cost of an eVTOL: The actual sale price of eVTOLs has not been disclosed by manufacturers. The two-seater eVTOL XPeng X2 is reported unofficially at 1 million RMB. We assume that eVTOL comprises a base cost plus a 50% premium and 400,000 RMB for maintenance. The eVTOL is set to operate 341 days each year for six years (two days for examination per month). Thus, the daily cost per eVTOL is approximately $\frac{1,000,000 \times 150\% + 400,000}{6 \times 341} \approx 928.7$ RMB/day

2. Daily Cost of shuttle vertiport: The base land cost for a vertiport is 1.4 million RMB using at least 20 years. Thus, the daily cost of each vertiport is $\frac{1,400,000}{20 \times 365} \approx 191.8$ RMB/day.

3. Daily Cost of a Landing Pad: Pads require unique construction and maintenance to ensure safe landings. The base cost is 900,000 RMB in ten years and the maintenance cost is 30,000 annually with 335 operating days. Thus, the daily cost for a pad is approximately $\frac{900,000}{10 \times 365} + \frac{30,000}{335} \approx 336.2$ RMB/day.

4. Flight Cost Per Kilometer: Autoflight's eVTOL can cruise 250 km on 160 degrees of electricity. UAM's operations will reach the third level of Beijing's electricity pricing at 0.78 RMB/kWh. Hence, the cost of electricity is 0.499 RMB/km. Considering that eVTOLs in airport shuttle service will not reach 250 km per trip and need multiple take-offs and landings, we adjusted the electricity cost to 130%. Thus, the flight energy cost is $0.78 \times \frac{160}{250} \times 120\% \approx 0.65$ RMB/km.

5. Charging for Passengers: We do not consider carpooling. Charge price is estimated by adding the base cost to the energy cost. We set the base cost at four times X2's sale price of 4 million. Meanwhile, the eVTOL will work for 6 years with 341 operating days each year. As the average shuttle distance to Beijing Capital Airport is 33.04 km, eVTOL may reach around 30 shuttles one day. Thus, the daily charge cost is $\frac{4,000,000}{6 \times 341 \times 33.04 \times 30} + 0.65 \approx 2.62$ RMB/km person.

6. Value of Travel Time: Typically, the value of travel time requires detailed surveys or data analysis. It will consider multiple factors such as income level, commuting modes, travel purpose, traffic conditions, and psychological factors. We estimated this value using the time and cost differences ratio between taxi and public transportation from the Amap. Additionally, considering discomfort or inconvenience during long-distance travel might affect the value of time, we adjusted it through linear regression. The analysis shows an excellent linear relationship between straight-line distance and the time value with significant at $P = 0.1$. The estimated time value is 1.98 RMB/km. As air travelers have higher time sensitivity, we increased this value by 25% to 2.5 RMB/km.

7. Cruising Speed: There is a significant variation in the speeds of different eVTOLs generally ranging from 100 km/h to 250 km/h. This paper selects four speeds for testing.

8. Number of Pads per Vertiport: This parameter is big enough to warrant a stress experiment to determine the optimal operational scale for a UAM shuttle vertiport. The findings will provide valuable guidance for maximizing network benefits in airport shuttle scenarios.

References

- Al Haddad, C., Chaniotakis, E., Straubinger, A., Plötner, K., Antoniou, C., 2020. Factors affecting the adoption and use of urban air mobility. *Transp. Res. A* 132, 696–712.
- Archer, 2022. Archer unveils its production aircraft, midnight. Available online at <https://archer.com/news/archer-unveils-its-production-aircraft-midnight>.
- Autoflight-Press, 2021. Autoflight. Available online at <https://autoflight.com/zh/press/>.
- Becker, K., Terekhov, I., Gollnick, V., 2018. A global gravity model for air passenger demand between city pairs and future interurban air mobility markets identification. In: 2018 Aviation Technology, Integration, and Operations Conference. p. 2885.
- Beijing Municipal Bureau of Economy and Information Technology, 2024. Action plan for promoting high-quality development of the low-altitude economy in Beijing. Available at: https://www.beijing.gov.cn/hudong/gfxwjz/jjxx/202405/t20240516_3685592.html. [Online; Accessed 26 June 2024]. Official Document.
- Berckman, L., Ajay, C., Kate, H., Tarun, D., Matt, S., 2022. Advanced air mobility: Achieving scale for value realization, midnight. Available online at <https://www2.deloitte.com/us/en/insights/industry/aerospace-defense/advanced-air-mobility-evtol-aircraft.html>.
- Biehle, T., 2022. Social sustainable urban air mobility in Europe. *Sustainability* 14 (15), 9312.
- Bierlaire, M., 1998. Discrete choice models. In: *Operations Research and Decision Aid Methodologies in Traffic and Transportation Management*. Springer, pp. 203–227.
- Binder, R., Garrow, L.A., German, B., Mokhtarian, P., Daskilewicz, M., Douthat, T.H., 2018. If you fly it, will commuters come? A survey to model demand for evtol urban air trips. In: 2018 Aviation Technology, Integration, and Operations Conference. p. 2882.
- Briefing, P., 2020. The impact of COVID-19 lockdowns on road deaths in april 2020. *Eur. Transp. Saf. Council* 1–21.
- Brunelli, M., Ditta, C.C., Postorino, M.N., 2023. SP surveys to estimate airport shuttle demand in an urban air mobility context. *Transp. Policy* 141, 129–139.
- Bulusu, V., Onat, E.B., Sengupta, R., Yedavalli, P., Macfarlane, J., 2021. A traffic demand analysis method for urban air mobility. *IEEE Trans. Intell. Transp. Syst.* 22 (9), 6039–6047.
- CAAC, 2024. Interim regulations for unmanned aircraft flight management. Available online at https://www.gov.cn/yaowen/liebiao/202306/content_6888833.htm.
- Chan, Y., Ng, K.K., Lee, C., Hsu, L.-T., Keung, K., 2023. Wind dynamic and energy-efficiency path planning for unmanned aerial vehicles in the lower-level airspace and urban air mobility context. *Sustain. Energy Technol. Assess.* 57, 103202.
- Cho, S.-H., Kim, M., 2022. Assessment of the environmental impact and policy responses for urban air mobility: A case study of seoul metropolitan area. *J. Clean. Prod.* 360, 132139.
- Choi, J.H., Park, Y., 2022. Exploring economic feasibility for airport shuttle service of urban air mobility (UAM). *Transp. Res. A* 162, 267–281.
- Cohen, A.P., Shaheen, S.A., Farrar, E.M., 2021. Urban air mobility: History, ecosystem, market potential, and challenges. *IEEE Trans. Intell. Transp. Syst.* 22 (9), 6074–6087.
- EASA, N., 2021. *Study on the societal acceptance of urban air mobility in Europe*.
- EASA, 2023. Flying in your country - national aviation authorities. Available online at <https://www.easa.europa.eu/en/domains/civil-drones/naa>.
- EHang-Intelligence, 2021. How does ehang intelligence lead the future of urban air mobility. Available online at <https://www.ehang.com/cn/news/737.html>.
- Feldhoff, E., Soares Roque, G., 2021. Determining infrastructure requirements for an air taxi service at cologne bonn airport. *CEAS Aeronaut. J.* 12 (4), 821–833.
- Fu, M., Straubinger, A., Schaumeier, J., 2022. Scenario-based demand assessment of urban air mobility in the greater Munich area. *J. Air Transp.* 30 (4), 125–136.
- Garrow, L.A., 2016. *Discrete Choice Modelling and Air Travel Demand: Theory and Applications*. Routledge.
- General Office of the People's Government of Beijing Municipality, 2023. Implementation plan for promoting innovation and development of future industries in Beijing. Available at: https://www.beijing.gov.cn/zhengce/zhengcefagui/202309/t20230908_3255227.html. [Online; Accessed 26 June 2024]. Official Document.
- Goyal, R., Reiche, C., Fernando, C., Serrao, J., Kimmel, S., Cohen, A., Shaheen, S., 2018. Urban Air Mobility (UAM) Market Study. Technical Report.
- Grandl, G., Ostgatthe, M., Cachay, J., Doppler, S., Salib, J., Ross, H., 2018. The future of vertical mobility. A Porsche consulting study.
- Greenfeld, I., 2019. Concept of Operations for Urban Air Mobility Command and Control Communications. Technical Report.
- Gudmundsson, H., Hall, R.P., Marsden, G., Zietsman, J., et al., 2016. Sustainable Transportation. Sprenger-Verlag Samf, Heidelberg, Ger. Frederiksberg, Denmark.
- Haan, J., Garrow, L.A., Marzuoli, A., Roy, S., Bierlaire, M., 2021. Are commuter air taxis coming to your city? A ranking of 40 cities in the United States. *Transp. Res. C* 132, 103392.
- Habitat, U., 2022. World cities report 2022: Envisaging the future of cities. United Nations Human Settlements Programme: Nairobi, Kenya 41–44.

- Hader, M., Baur, S., Kopera, S., Schönberg, T., Hasenberg, J.-P., 2020. Urban Air Mobility: USD 90 Billion of Potential: How to Capture a Share of the Passenger Drone Market. Roland Berger.
- Hamilton, B.A., 2018. Urban Air Mobility (UAM) Market Study–Technical Outbrief. National Aeronautics and Space Administration (NASA).
- Heidorn, C., 2018. Manual on the basic set of environment statistics.
- Hill, B.P., DeCarme, D., Metcalfe, M., Griffin, C., Wiggins, S., Metts, C., Bastedo, B., Patterson, M.D., Mendonca, N.L., 2020. UAM vision concept of operations (CONOPS) UAM maturity level (UML) 4.
- Holden, J., Goel, N., 2016. Fast-Forwarding to a Future of On-Demand Urban Air Transportation. San Francisco, CA.
- Husemann, M., Kirste, A., Stumpf, E., 2023. Analysis of cost-efficient urban air mobility systems: Optimization of operational and configurational fleet decisions. European J. Oper. Res.
- Hwang, J.-H., Hong, S., 2023. A study on the factors influencing the adoption of urban air mobility and the future demand: Using the stated preference survey for three UAM operational scenarios in South Korea. J. Air Transp. Manage. 112, 102467.
- IEA, 2020. Global energy review 2020. <https://www.iea.org/reports/global-energy-review-2020>.
- Joby-Aviation, 2023. Joby begins flight testing with pilot on board. Available online at <https://www.jobyaviation.com/news/joby-begins-flight-testing-pilot-on-board/>.
- Joby-Certification, 2024. Joby completes third stage of FAA certification process. Available online at <https://www.jobyaviation.com/news/joby-completes-third-stage-faa-certification-process/>.
- Joby-Noise, 2022. Joby confirms revolutionary low noise footprint following NASA testing. Available online at <https://www.jobyaviation.com/news/joby-revolutionary-low-noise-footprint-nasa-testing/>.
- Joby-UAE, 2024. Joby to launch air taxi service in UAE. Available online at <https://www.jobyaviation.com/news/joby-to-launch-air-taxi-service-uae/>.
- Johnston, T., Riedel, R., Sahdev, S., 2020. To take off, flying vehicles first need places to land. McKinsey Cent. Future Mobil. 2–8.
- Kim, S.H., 2019. Receding horizon scheduling of on-demand urban air mobility with heterogeneous fleet. IEEE Trans. Aerosp. Electron. Syst. 56 (4), 2751–2761.
- Kleinbekman, I.C., Mitici, M., Wei, P., 2020. Rolling-horizon electric vertical takeoff and landing arrival scheduling for on-demand urban air mobility. J. Aerosp. Inf. Syst. 17 (3), 150–159.
- Lewis, E., Ponnock, J., Cherqaoui, Q., Holmdahl, S., Johnson, Y., Wong, A., Gao, H.O., 2021. Architecting urban air mobility airport shuttling systems with case studies: Atlanta, Los Angeles, and Dallas. Transp. Res. A 150, 423–444.
- Mayor, T., Anderson, J., 2019. Getting mobility off the ground. KPMG Insight Available online at <https://institutes.kpmg.us/content/dam/advisory/en/pdfs/2019/urban-airmobility.pdf>. (Accessed 2 September 2020).
- McKinsey, 2022. Perspectives on Advanced Air Mobility. Report.
- NASA, 2023. NASA, joby pave the way for air taxis in busy airports. Available online at <https://www.nasa.gov/aeronautics/nasa-joby-pave-the-way-for-air-taxis-in-busy-airports/>.
- National Academies of Sciences, E., Medicine, et al., 2020. Advancing Aerial Mobility: A National Blueprint. National Academies Press.
- NATS, 2023. Pioneering air traffic control simulations pave the way for eVTOL operations. Available online at <https://www.nats.aero/news/pioneering-air-traffic-control-simulations-pave-the-way-for-evtol-operations/>.
- Okamoto, H., Makino, H., 2007. Management of congestion in Japan. In: 23RD Piarc World Road Congress Paris, 17-21 September 2007.
- Peng, X., Bulusu, V., Sengupta, R., 2022. Hierarchical vertiport network design for on-demand multi-modal urban air mobility. In: 2022 IEEE/AIAA 41st Digital Avionics Systems Conference. DASC, IEEE, pp. 1–8.
- Rassafi, A., Vaziri, M., 2005. Sustainable transport indicators: definition and integration. Int. J. Environ. Sci. Technol. 2, 83–96.
- Rath, S., Chow, J.Y., 2022. Air taxi skyport location problem with single-allocation choice-constrained elastic demand for airport access. J. Air Transp. Manage. 105, 102294.
- Ravich, T.M., 2019. On-demand aviation: Governance challenges of urban air mobility (“UAM”). Penn State Law Rev. 124, 657.
- Ribeiro, J.K., Borille, G.M.R., Caetano, M., da Silva, E.J., 2023. Repurposing urban air mobility infrastructure for sustainable transportation in metropolitan cities: A case study of vertiports in São Paulo, Brazil. Sustainable Cities Soc. 98, 104797.
- Rimjha, M., Hotle, S., Trani, A., Hinze, N., 2021a. Commuter demand estimation and feasibility assessment for urban air mobility in northern California. Transp. Res. A 148, 506–524.
- Rimjha, M., Hotle, S., Trani, A., Hinze, N., Smith, J.C., 2021b. Urban air mobility demand estimation for airport access: A Los Angeles international airport case study. In: 2021 Integrated Communications Navigation and Surveillance Conference. ICNS, IEEE, pp. 1–15.
- Robinson, J.N., Sokollek, M.-D.R., Justin, C.Y., Mavris, D.N., 2018. Development of a methodology for parametric analysis of STOL airpark geo-density. In: 2018 Aviation Technology, Integration, and Operations Conference. p. 3054.
- Roy, S., Kotwicz Herniczek, M.T., German, B.J., Garrow, L.A., 2021. User base estimation methodology for a business airport shuttle air taxi service. J. Air Transp. 29 (2), 69–79.
- Roy, S., Kotwicz Herniczek, M.T., Leonard, C., German, B.J., Garrow, L.A., 2022. Flight scheduling and fleet sizing for an airport shuttle air taxi service. J. Air Transp. 30 (2), 49–58.
- Shaheen, S., Cohen, A., Farrar, E., 2018. The potential societal barriers of urban air mobility (UAM).
- Straubinger, A., Rothfeld, R., Shamiyah, M., Büchter, K.-D., Kaiser, J., Plötner, K.O., 2020. An overview of current research and developments in urban air mobility–Setting the scene for UAM introduction. J. Air Transp. Manage. 87, 101852.
- Tarafdar, S., Rimjha, M., Hinze, N., Hotle, S., Trani, A.A., 2019. Urban air mobility regional landing site feasibility and fare model analysis in the greater northern California region. In: 2019 Integrated Communications, Navigation and Surveillance Conference. ICNS, IEEE, pp. 1–11.
- UAS-Maps, 2023. UAS facility map. Available: https://www.faa.gov/uas/commercial_operators/uas_facility_maps.
- UrbanV, 2024. UrbanV chooses euthalia to protect and secure its vertiports against adverse weather conditions. Available online at <https://www.urbanv.com/en/urbanv-chooses-euthalia-to-protect-and-secure-its-vertiports-against-adverse-weather-conditions/>.
- Vascik, P.D., Hansman, R.J., 2017. Evaluation of key operational constraints affecting on-demand mobility for aviation in the Los Angeles basin: ground infrastructure, air traffic control and noise. In: 17th AIAA Aviation Technology, Integration, and Operations Conference. p. 3084.
- Vascik, P.D., Hansman, R.J., Dunn, N.S., 2018. Analysis of urban air mobility operational constraints. J. Air Transp. 26 (4), 133–146.
- Vempati, L., Geffard, M.V., Anderegg, A., 2022. Challenges and decisions for near-term integration of urban air mobility (UAM) operations. In: AIAA Aviation 2022 Forum. p. 3402.
- Venkatesh, N., Payan, A.P., Justin, C.Y., Kee, E., Mavris, D., 2020. Optimal siting of sub-urban air mobility (suam) ground architectures using network flow formulation. In: AIAA AVIATION 2020 FORUM. p. 2921.
- Vertical Flight Society, 2023. eVTOL aircraft directory. <https://evtol.news/aircraft>. [Online; Accessed 26 June 2024].
- Volocopter, 2022. M3 systems, pipistrel, and volocopter complete deconfliction flight tests in France. Available online at <https://www.volocopter.com/en/newsroom/volocopter-m3-systems-and-pipistrel-complete-deconfliction-flight-tests-in-france>.
- Volocopter-Paris, 2023. Groupe ADP & volocopter at forefront of electric urban air mobility: A world first in summer 2024. Available online at <https://www.volocopter.com/en/newsroom/volocopter-paris-routes>.
- Volocopter-POA, 2024. Volocopter receives green light for VoloCity serial production. Available online at <https://www.volocopter.com/en/newsroom/vc-poа-extension>.

- Wai, C.W., Tan, K., Low, K.H., 2021. Preliminary study of transport pattern and demand in Singapore for future urban air mobility. In: AIAA Scitech 2021 Forum. p. 1633.
- Wang, Z., Delahaye, D., Farges, J.-L., Alam, S., 2022a. Complexity optimal air traffic assignment in multi-layer transport network for urban air mobility operations. *Transp. Res. C* 142, 103776.
- Wang, K., Jacquillat, A., Vaze, V., 2022b. Vertiport planning for urban aerial mobility: an adaptive discretization approach. *Manuf. Serv. Oper. Manage.* 24 (6), 3215–3235.
- Wang, K., Qu, X., 2023. Urban aerial mobility: Reshaping the future of urban transportation. *Innovation* 4 (2).
- Wei, L., Justin, C.Y., Mavris, D.N., 2020. Optimal placement of airparks for STOL urban and suburban air mobility. In: AIAA Scitech 2020 Forum. p. 0976.
- Wei, Q., Nilsson, G., Coogan, S., 2021. Scheduling of urban air mobility services with limited landing capacity and uncertain travel times. In: 2021 American Control Conference. ACC, IEEE, pp. 1681–1686.
- Wei, Q., Nilsson, G., Coogan, S., 2022. Safety verification for urban air mobility scheduling. *IFAC-PapersOnLine* 55 (13), 306–311.
- Willey, L.C., Salmon, J.L., 2021. A method for urban air mobility network design using hub location and subgraph isomorphism. *Transp. Res. C* 125, 102997.
- Wu, Z., Zhang, Y., 2020. Optimal eVTOL charging and passenger serving scheduling for on-demand urban air mobility. In: AIAA Aviation 2020 Forum. p. 3253.
- Xing, J., Takahashi, H., Kameoka, H., 2010. Mitigation of expressway traffic congestion through transportation demand management with toll discount. *IET Intell. Transp. Syst.* 4 (1), 50–60.
- Yedavalli, P., Mooberry, J., 2019. An assessment of public perception of urban air mobility (UAM). *Airbus UTM: Defin. Future Skies* 2046738072–1580045281.
- Zhou, H., Gao, H., 2020. The impact of urban morphology on urban transportation mode: A case study of Tokyo. *Case Stud. Transp. Policy* 8 (1), 197–205.